Exceptional Event Demonstration for Ozone Exceedances in Clark County, Nevada: July 25–27, 2018

September 2021

Clark County Department of Environment and Sustainability
4701 West Russell Road, Suite 200
Las Vegas, NV 89118
(702) 455-5942

TABLE OF CONTENTS

LIST OF FIGURES

LIST OF TABLES

1.0 OVERVIEW

1.1 INTRODUCTION

Ozone (O_3) exceedances in Clark County are frequently influenced by surrounding wildfires. In the proper weather conditions, wildfire emissions can travel hundreds of miles from the point of origin. This is especially true of wildfires in California, which cause more exceedances of the National Ambient Air Quality Standard (NAAQS) for ozone in Clark County than fires in other areas because of regionally predominant winds that flow from California to the Las Vegas Valley (LVV) in summer.

Figure 1-1 uses data from annual "Wildland Fire Summary" reports (2014–2018) from the National Interagency Coordination Center (NICC) to show the strong relationship between the number of ozone exceedance days in Clark County and the total area in California burned by wildfires ($R^2 = 0.9091$). The 2018 fire season in California was the most destructive on record, with the NICC reporting a total of 8,054 fires burning an area of 1,823,153 acres. Figure 1-2 shows the high correlation between the area burned (logarithmic value) in California and the number of ozone exceedance days in Clark County from May to August 2018 ($R^2 = 0.9591$), based on the "2018 Wildfire Activity Statistics" report published by the California Department of Forestry and Fire Protection (CAL FIRE). Though it represents only the areas of the state for which CAL FIRE was responsible, that was more than 50% of the total burned area in California.

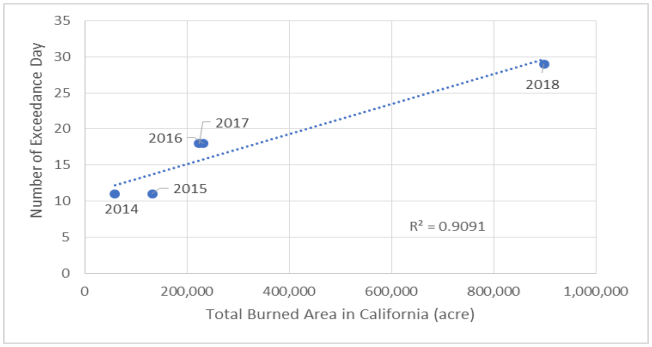

Figure 1-1. Relationship between Total Burned Area in California and Number of Exceedance Days in Clark County in Summer Months (May–August), 2014–2018.

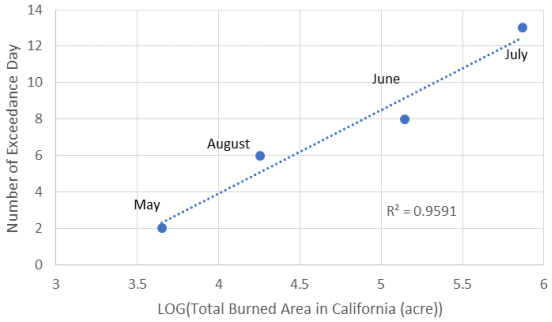

Figure 1-2. Relationship between Log Value of Total Burned Area and Number of Exceedance Days in Summer Months of 2018.

With that background in mind, the Clark County Department of Environment and Sustainability (DES) is concurrently submitting several exceptional events demonstrations of ozone concentrations that exceeded the 2015 ozone NAAQS due to smoke impact on the days in 2018 listed in Table 1-1. All have been prepared consistent with Title 40, Part 50 of the Code of Federal Regulations (40 CFR 50).

This document is submitted for July 25-27, 2018, events influenced by smoke from the Ferguson Fire, Georges Fire, Lions Fire, Cranston Fire in California, and other unnamed wildfires in California/Mexico border areas.

The submittal process began with an Exceptional Events Initial Notification sent to EPA Region 9 on November 30, 2020 (Appendix A). With this demonstration package, DES petitions the Regional Administrator for Region 9 of the U.S. Environmental Protection Agency (EPA) to exclude air quality monitoring data for ozone on July 25—27, 2018, from the normal planning and regulatory requirements under the Clean Air Act (CAA) in accordance with the Exceptional Events Rule (EER), codified at 40 CFR 50.1, 50.14, and 51.930.

Table 1-1 lists the maximum daily 8-hour average of ozone (MDA8 ozone) at network monitors on the exceedance days.

Table 1-1. Ozone Monitors Proposed for Data Exclusion

AQSID[1]	320030043	320030071	320030073	320030075	320030298	320030540
Date	Paul Meyer	Walter Johnson	Palo Verde	Joe Neal	Green Valley	Jerome Mack
20180619[2]	72 (10)	72 (14)	—	—	77 (4)	75 (4)
20180620	71 (15)	74 (9)	—	72 (10)	—	—
20180623	72 (7)	76 (4)	71 (5)	72 (9)	75 (6)	72 (10)
20180627	75 (4)	76 (4)	72 (3)	72 (8)	78 (1)	76 (3)
20180714	72 (13)	—	—	—	78 (3)	78 (1)
20180715	—	71 (21)	—	78 (2)	73 (11)	73 (7)
20180716	75 (3)	79 (1)	75 (1)	80 (1)	71 (19)	73 (8)
20180717	74 (5)	77 (3)	74 (2)	—	—	—
20180725	71 (17)	72 (15)	—	—	72 (14)	—
20180726	72 (8)	75 (6)	70 (6)	—	77 (4)	77 (2)
20180727	72 (9)	74 (11)	70 (7)	76 (4)	—	—
20180730	—	—	—	—	73 (11)	72 (11)
20180731	—	73 (13)	—	73 (6)	—	—
20180806	79 (1)	77 (2)	72 (4)	76 (3)	74 (10)	71 (12)
20180807	73 (6)	74 (7)	—	74 (5)	72 (16)	71 (13)

[1]Air Quality System identification numbers (AQSID) and local names identify key monitors.
[2]MDA8 ozone is listed in parts per billion (ppb) with Tier 2, Key Factor 2 ranking of measurement for 2018 season in parentheses.

1.2 EXCEPTIONAL EVENT DEMONSTRATION CRITERIA

40 CFR 50.1(j) states:

> *Exceptional event* means an event(s) and its resulting emissions that affect air quality in such a way that there exists a clear causal relationship between the specific event(s) and the monitored exceedance(s) or violation(s), is not reasonably controllable or preventable, is an event(s) caused by human activity that is unlikely to recur at a particular location or a natural event(s), and is determined by the Administrator in accordance with 40 CFR 50.14 to be an exceptional event.

40 CFR 50.14(c)(1)(i) requires that air agencies must "notify the public promptly whenever an event occurs or is reasonably anticipated to occur which may result in the exceedance of an applicable air quality standard" in accordance with the mitigation requirement at 40 CFR 51.930(a)(1). Details on DES's public notification can be found in Appendix B.

As specified in 40 CFR 50.14(c)(3)(iv), the following elements must be included to justify the exclusion of air quality data from a NAAQS determination:

1. A narrative conceptual model that describes the event(s) causing the exceedance or violation and a discussion of how emissions from the event(s) led to the exceedance or violation at the affected monitor(s).

2. A demonstration that the event affected air quality in such a way that there exists a clear causal relationship between the specific event and the monitored exceedance or violation.

3. Analyses comparing the claimed event-influenced concentration(s) to concentrations at the same monitoring site at other times. However, the EPA Administrator is restricted from requiring a state to prove a specific percentile point in the distribution of data.

4. A demonstration that the event was both not reasonably controllable and not reasonably preventable.

5. A demonstration that the event was a human activity that is unlikely to recur at a particular location, or was a natural event.

"EPA Guidance on the Preparation of Exceptional Events Demonstration for Wildfire Events that May Influence Ozone Concentrations" (EPA 2016) describes a three-tier analysis approach to determine a "clear causal relationship" for exceptional events, which is summarized below. Section 4 of this document, "Clear Causal Relationship," provides the details of these analyses.

Tier 1:
Key factors for this tier are exceedances out of the normal ozone season and/or concentrations that are 5–10 ppb greater than non-event-related concentrations.

Tier 2:
There are two key factors for this tier: fire emissions & distance (Q/d) and comparison of event ozone concentrations to non-event high-ozone concentrations. Q/d analysis for August 6, the day with the highest smoke impact in 2018: Even with the contribution from the three largest and two smaller wildfires, the Q/d threshold could not be achieved due to the significant distance between Las Vegas and the wildfires' origin points. Since even the worst-case event failed to meet the Q/d threshold, it seemed pointless to perform this analysis for other, lesser wildfire events.

This tier may include additional analyses of smoke maps, plume trajectories, satellite retrievals, sounding data, and time series of supporting ground measurements to provide evidence of wildfire emissions transported to local monitors.

Tier 3:
This tier involves statistical modeling of MDA8 ozone concentrations using generalized additive models (GAMs) to assess wildfire influences on local ozone concentrations.

DES has prepared this package to meet the requirements for seeking EPA concurrence for data exclusion.

This exceptional event demonstration will undergo a 30-day public comment period concurrent with EPA's review beginning September 3, 2021. A copy of the public notice, along with any comments received and responses to those comments, will be submitted to EPA after the comment period has closed, consistent with the requirements of 40 CFR 50.14(c)(3)(v). Appendix C documents the public comment process.

1.3 REGULATORY SIGNIFICANCE OF THE EXCLUSION

The LVV, located within Clark County, Nevada, is currently designated as a nonattainment area for the 2015 ozone NAAQS of 70 ppb. Table 1-2 lists the 4th highest 8-hour average ozone recorded at the monitors listed in Table 1-1—including wildfire days in 2018 and excluding wildfire days in 2020—for the most recent three-year period (2018–2020), along with the resulting design value (DV) for each monitor. The table also shows the 4th highest 8-hour average ozone and DVs for 2018 after the requested exceedance days are excluded from the DV calculation (the shaded columns). Since the recalculated DVs meet the 2015 NAAQS, the valley would be reclassified as "attainment" if EPA concurs with this demonstration. EPA concurrence will thus have a significant impact on DES's attainment of the 2015 ozone NAAQS.

Table 1-2. Impact of Wildfire Events on Design Values of 2018–2020 (all values in ppb)

Site Name	Fourth Highest Average			Current	Wildfire Days Excluded	
	2018	2019	2020[1]	Design Value	2018	Design Value
Jerome Mack	75	66	67	69	72	68
Paul Meyer	75	69	70	71	71	70
Joe Neal	76	68	68	70	71	69
Walter Johnson	76	68	70	71	73	70
Palo Verde	72	62	67	67	68	65
Green Valley	77	70	68	71	72	70

[1] Assume wildfire days are excluded.

2.0 AREA DESCRIPTION AND CHARACTERISTICS OF NON-EVENT OZONE FORMATION

2.1 AREA DESCRIPTION

Clark County covers 8,091 square miles at the southern tip of Nevada and has a population of over 2.2 million.[1] More than 95% of the county's residents live in the Las Vegas Valley, which is part of the Mojave Desert and constitutes Hydrographic Area (HA) 212. The valley encompasses about 1,600 km^2 and is surrounded by mountains extending 2,000–10,000 feet above its floor (Figure 2-1). The valley slopes downward from west to east (approximately 900 to 500 m above mean sea level), which affects the local climatology by driving variations in wind, temperature, and precipitation.

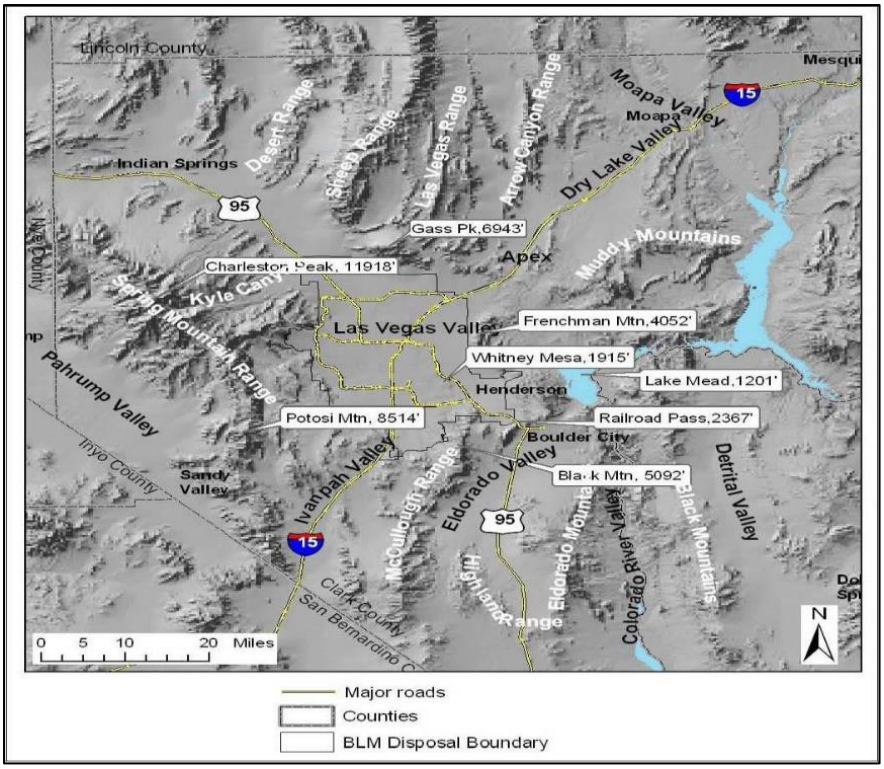

Figure 2-1. Mountain Ranges and Hydrographic Areas Surrounding the Las Vegas Valley.

Valley weather is characterized by low rainfall, hot summers, and mild winters. On average, June is the driest month; monsoons from the Gulf of California increase the humidity and cloud cover in July and August. The Interstate 15 (I-15) corridor through the Mojave Desert and Cajon Pass links Las Vegas with the eastern Los Angeles Basin, about 275 km to the southwest. This corridor is a potential pathway for the export of pollution from Los Angeles to the Mojave Desert and the LVV.

[1] *Clark County, Nevada 2017 Population Estimates*. Clark County (NV) Department of Comprehensive Planning.

Figure 2-2 shows the locations of Clark County ozone monitors. Most of the stations—Paul Meyer (PM), Walter Johnson (WJ), Palo Verde (PV), Joe Neal (JO), Jerome Mack (JM), and Green Valley (GV)—are in the populated areas of the valley (HA 212), but there are outlying stations in Apex, Mesquite, Boulder City, Jean, and Indian Springs. A station at the Spring Mountain Youth Camp was operated as a special purpose monitoring site for part of the 2018 ozone season.

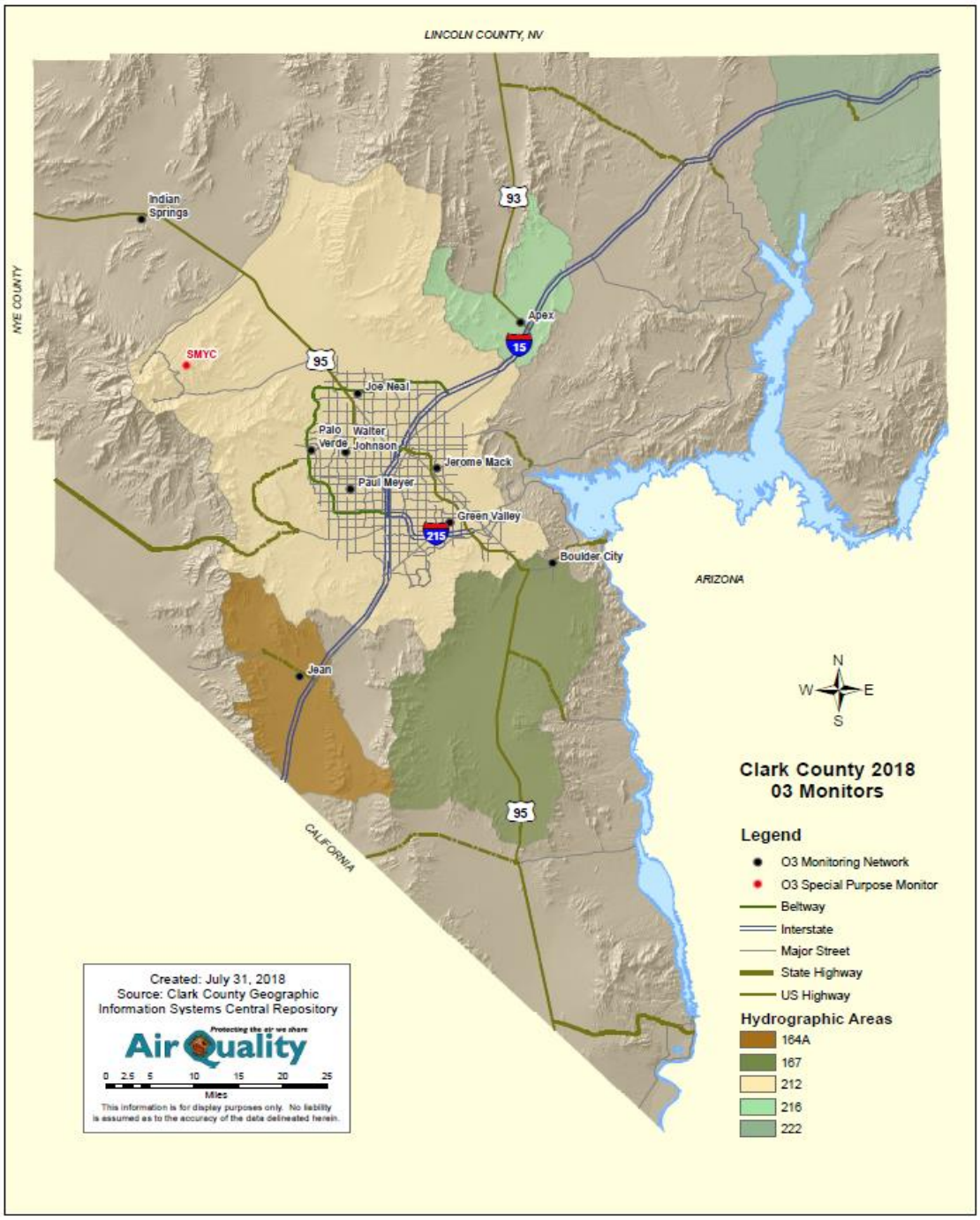

Figure 2-2. Clark County O_3 Monitoring Network.

Figures 2-3 and 2-4 show the locations of Clark County's Federal Equivalent Method (FEM) and Federal Reference Method (FRM) $PM_{2.5}$ monitors, respectively. Most of the stations are located in the populated areas of HA 212, with one outlying station in Jean, Nevada. Jean is considered a regional background site because it is located far enough from the valley to avoid impacts from local emissions. It is upwind of the Las Vegas Valley, but downwind of southern California.

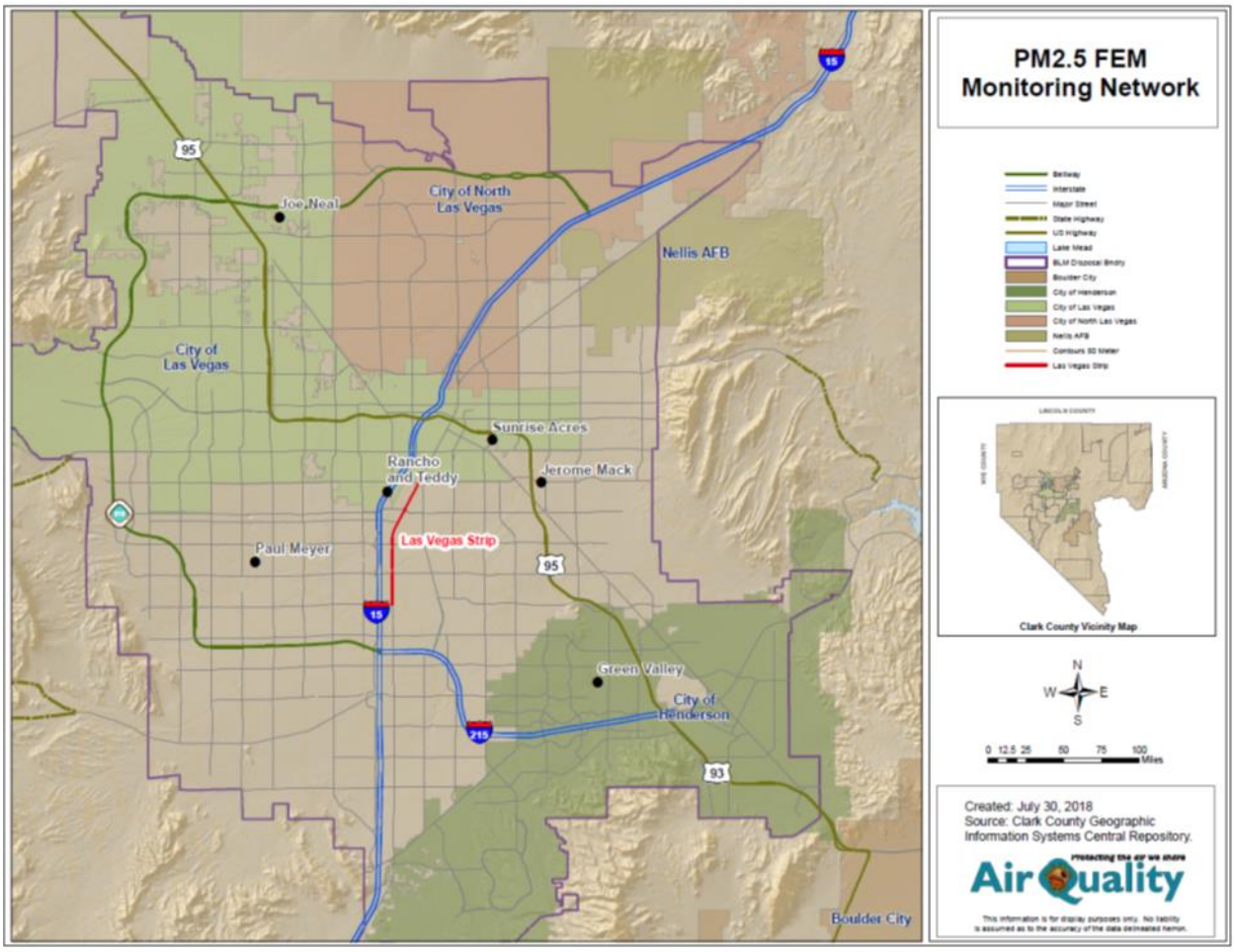

Figure 2-3. Locations of FEM $PM_{2.5}$ Monitors.

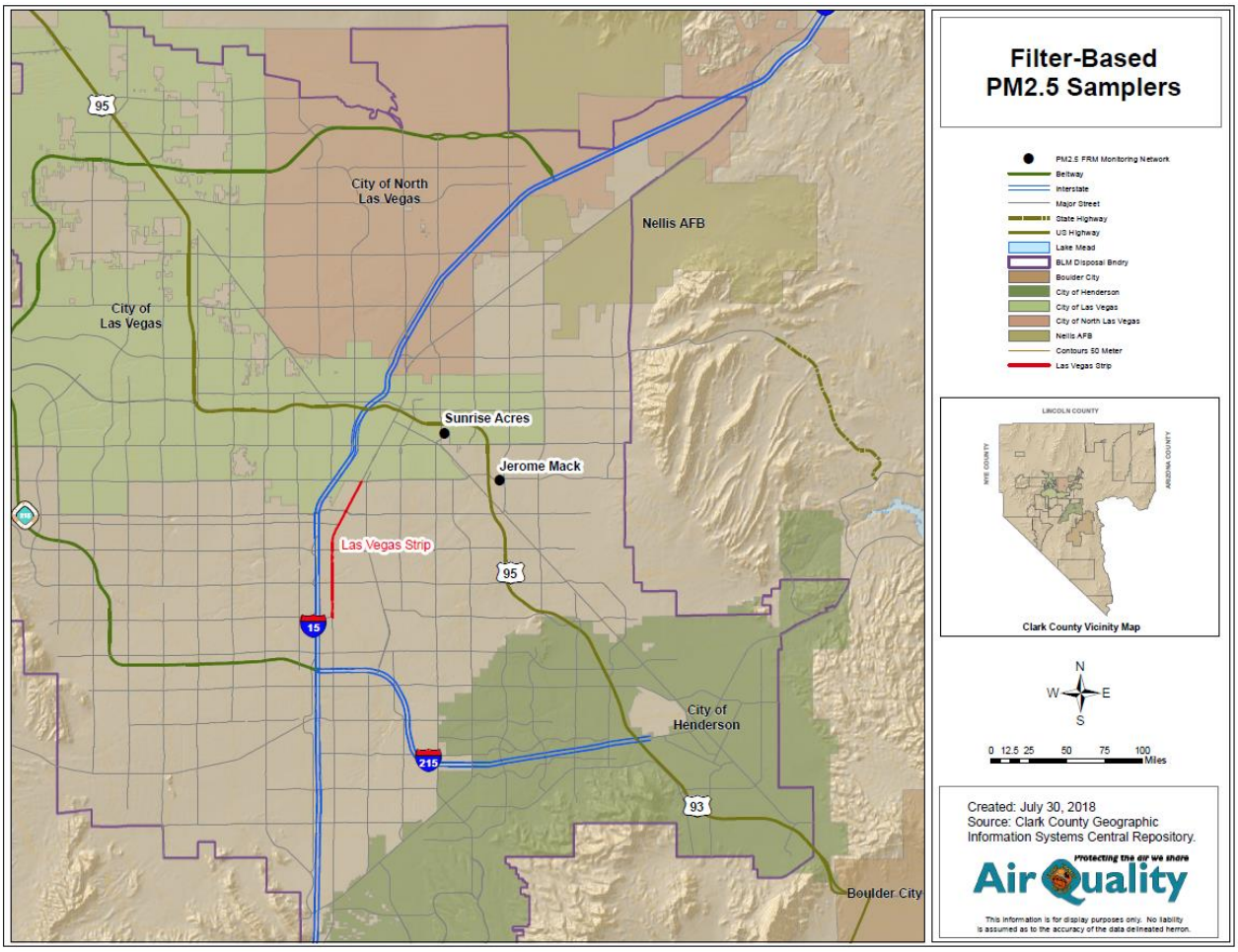

Figure 2-4. Locations of FRM $PM_{2.5}$ Monitors.

2.2 CHARACTERISTICS OF NON-EVENT OZONE FORMATION

Ozone, a secondary pollutant, is formed by complex processes in the interaction of nitrogen oxides (NO_x), volatile organic compounds (VOCs), temperature, and the intensity of solar radiation. The elevated ozone in the Las Vegas Valley can be characterized as the result of a combination of locally produced ozone under relatively stagnant conditions and different degrees of regional transport from upwind source areas, mainly in California.

2.2.1 Emission Trend

Mobile emission is the largest source of ozone precursors in Clark County. The area adjacent to two major transportation routes, I-15 and U.S. Highway 95, registers the highest emissions in the LVV. Figures 2-5 and 2-6 illustrate the county's ozone planning inventory for NO_x and VOC emissions, respectively, on a typical summer weekday. Throughout the years, ozone has decreased dramatically across much of the eastern United States over the last two decades (He et al.

2013; Lefohn et al. 2010), largely as a result of stricter emission controls on stationary and mobile NO_x sources (Butler et al. 2011; EPA 2012). These same reductions can be seen in California and Clark County.

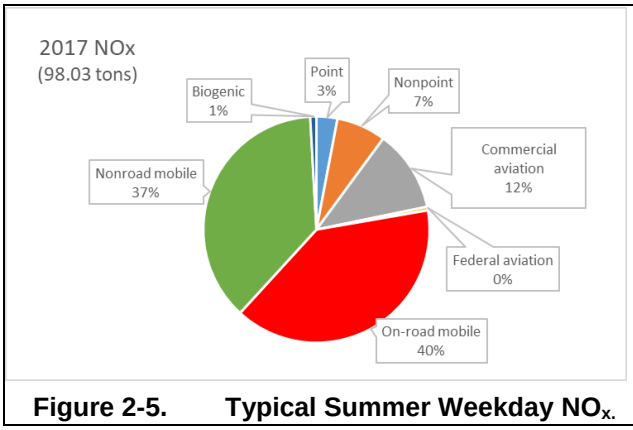

Figure 2-5. Typical Summer Weekday NO_x.

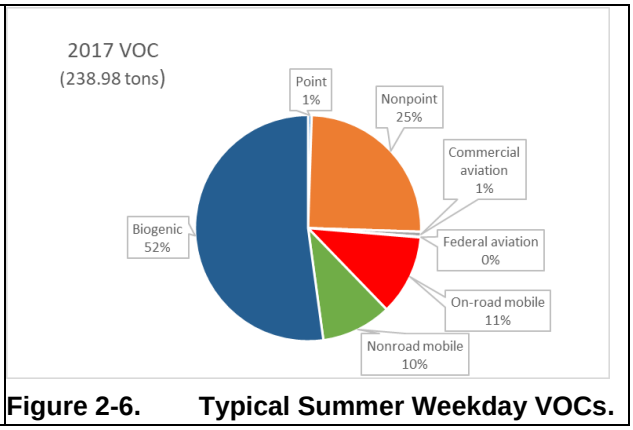

Figure 2-6. Typical Summer Weekday VOCs.

Source: https://www.clarkcountynv.gov/Environmental%20Sustainability/SIP%20Related%20Documents/O3/20200901_2015_O3_EI_ES_SIP_with_Appendices.pdf?t=1619706653363.

Figure 2-7 shows the downward trends of NO_x and VOC anthropogenic emissions in California from 1990–2019.

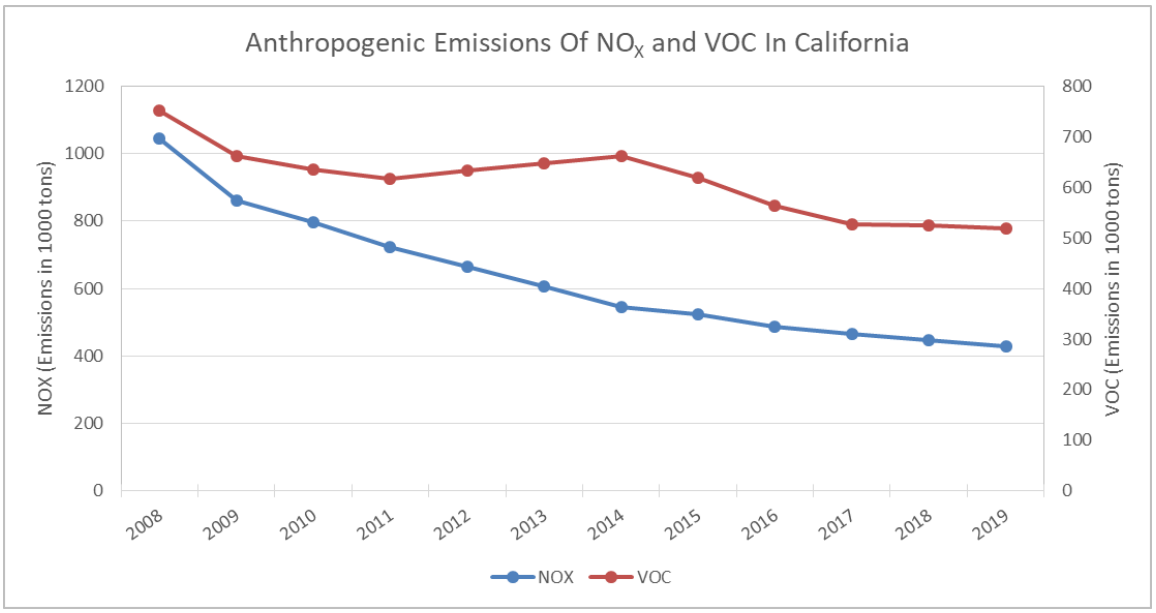

Source: https://www.epa.gov/air-emissions-inventories/air-pollutant-emissions-trends-data (under *State Annual Emissions Trend*).

Figure 2-7. Anthropogenic Emission Trends of NO_x and VOC in California, 2008–2019.

Figure 2-8 shows a downward trend in NO_x emissions and a slight increase in VOC anthropogenic emissions in Clark County from 2008–2017.

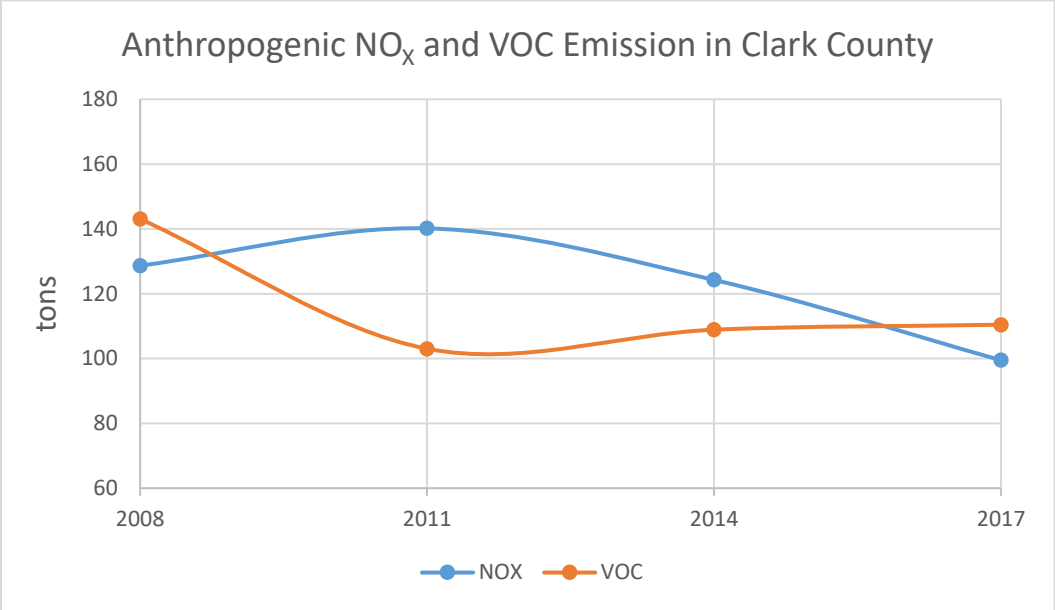

Source: https://www.epa.gov/air-emissions-inventories/national-emissions-inventory-nei.

Figure 2-8. Anthropogenic Emission Trends of NO_x and VOCs in Clark County, 2008–2017.

After a substantial reduction in NO_x emissions (approximately 55% in California and 25% locally) over the past 10 years, Figure 2-9 illustrates how the eight-hour ozone 4th highest averages in Clark County generally trended downward from 2009–2019 (except in 2018).

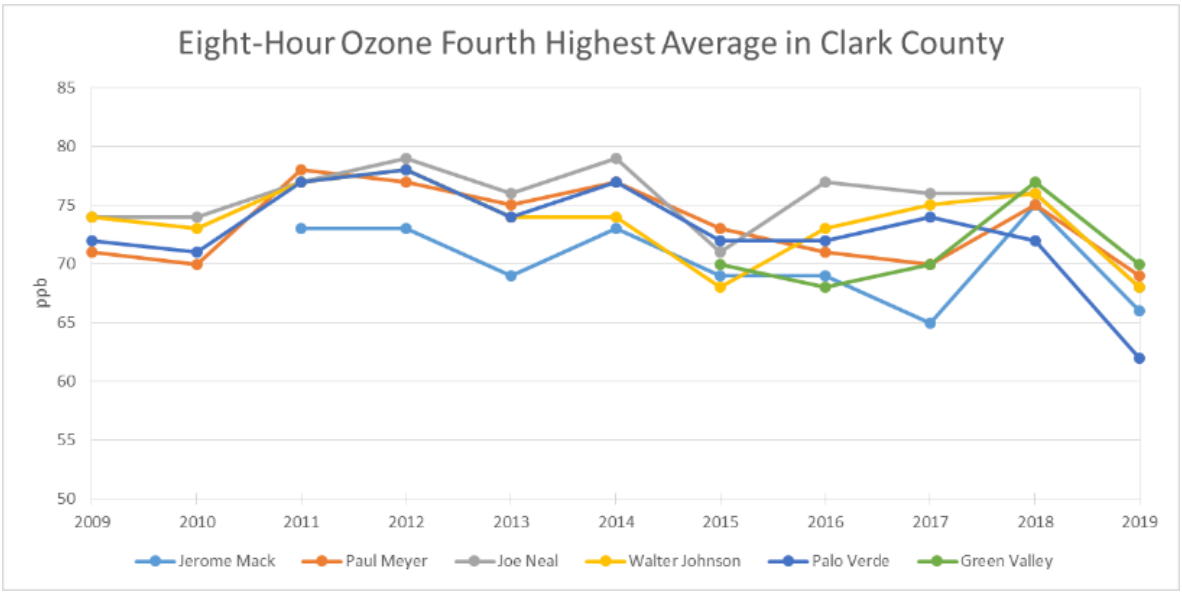

Figure 2-9. Eight-hour Ozone 4th Highest Average at Monitors in Clark County, 2009–2019.

2.2.2 Weather Patterns Leading to Ozone Formation

Most of the high ozone days in the Las Vegas Valley occur from May through August. During these months, warmer temperatures lead to the development of regional-scale southwest-north-east plains-mountain circulations and locally-driven valley and slope flows (Stewart et al. 2002). In general, winds during the nocturnal regime are dominated by downslope flows from the east and southwest converging into Las Vegas; downslope flows have also been observed northeast of the Spring Mountain Range. Southeasterly to southerly wind flow develops during the morning transition period, but the winds shift to the southwest by mid-afternoon as the mixed layer grows in depth and plains-mountain winds develop, driven by the thermal contrast between the land and the Gulf of California. This regional-scale flow converges with southeasterly up-valley flow in the Las Vegas Valley, and these winds typically persist until well into the night, when the nocturnal regime prevails again.

The convergence of afternoon southwesterly plain-mountain and southeasterly up-valley flows at the northwestern terminus of the valley frequently results in elevated ozone levels at JO and WJ. Figure 2-10 illustrates the typical ozone season (May–August) diurnal ozone patterns at the 50th and 95th percentiles at all monitors in HA 212. These patterns are based on historic ozone data from 2014–2018.

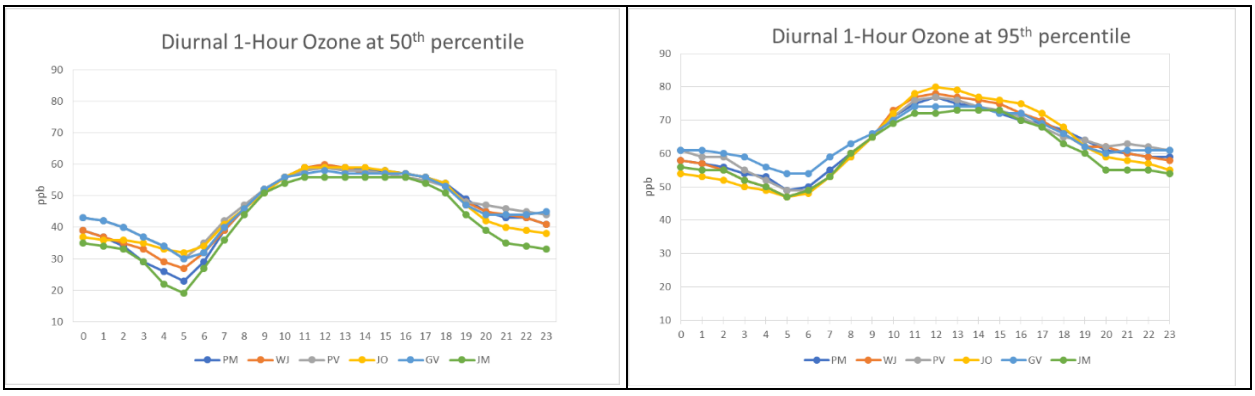

Figure 2-10. Typical Ozone Season 1-Hour Ozone Diurnal Pattern for 50th and 95th Percentile Values at Clark County Monitors.

2.2.3 Weekday and Weekend Effect

Figure 2-11 depicts air quality monitors in the LVV; the NO_2 monitors at Rancho Teddy (RT), Casino Center (CC), Sunrise Acres (SA), JM, and JO are marked as red dots. Most anthropogenic precursors are emitted from the urban core and follow a diurnal pattern related to traffic patterns, which peak twice daily at the morning and evening rush hours (Figure 2-12).

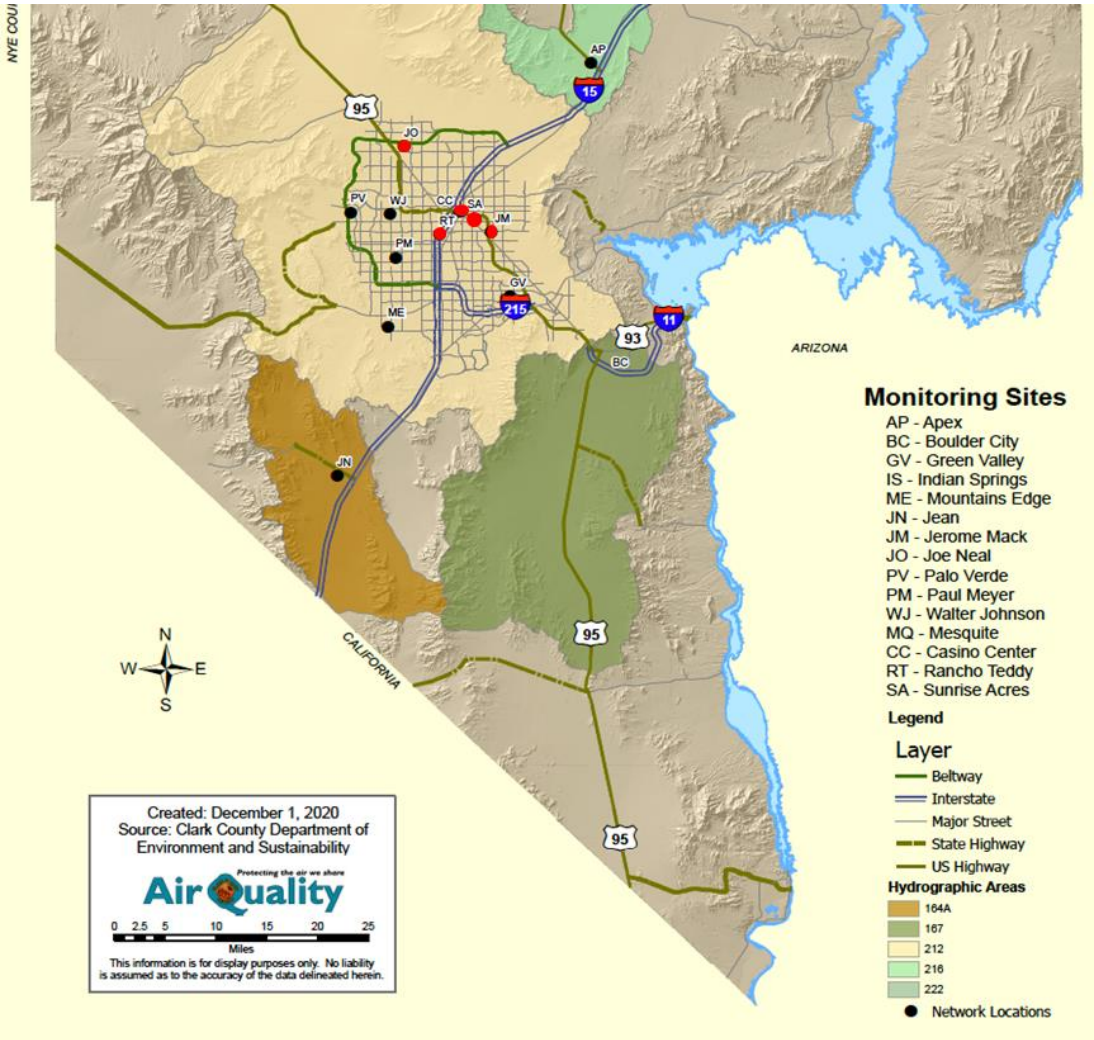

Note: Red dots = NO_2 monitors.

Figure 2-11. Locations of NO_2 Monitors.

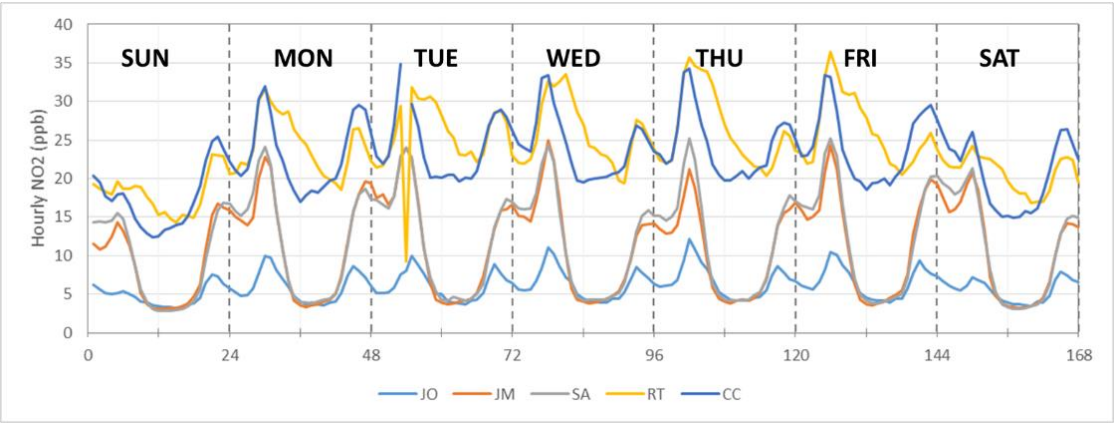

Figure 2-12. Weekly Pattern for 1-Hour NO_2 at Monitors from 2014–2019 (May–August).

Figure 2-13 shows that daily average NO_2 concentrations are lower on weekends than weekdays. The highest NO_2 concentrations are at RT and CC (urban core-downtown), and the lowest are at JO (further downwind). These weekly patterns are based on historic hourly and daily NO_2 concentrations recorded between 2014 and 2019 (May–August).

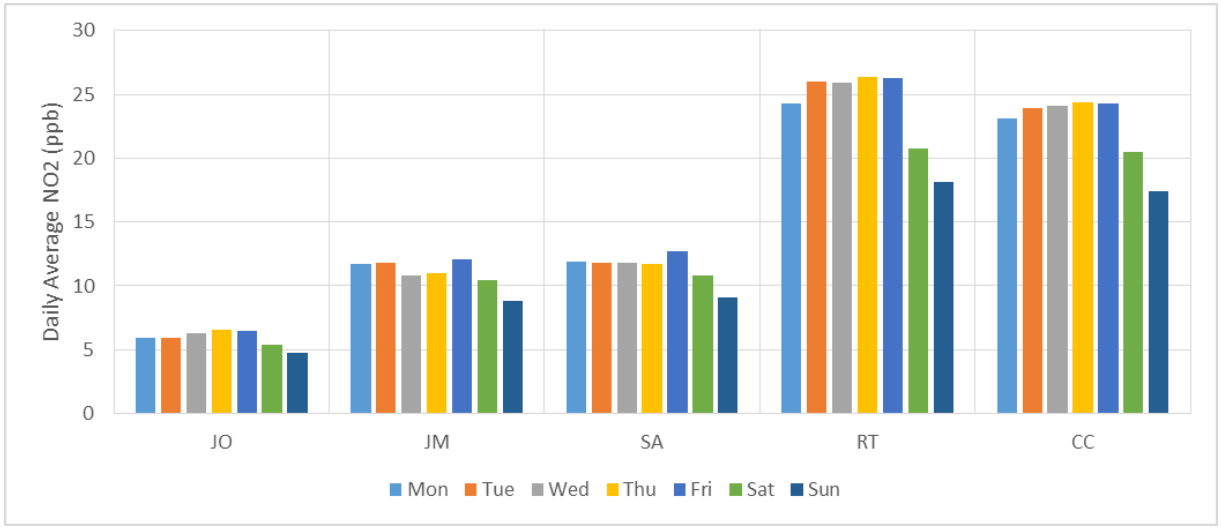

Figure 2-13. Weekly Pattern for 24-Hour NO_2 Average at Monitors from 2014–2019 (May–August).

Figure 2-14 shows the mean MDA8 O_3 at six monitors in HA 212 (see Figure 2-2) and the upwind monitor at Jean. It shows these sites have a similar weekly pattern, with the highest MDA8 O_3 on Fridays and Saturdays despite significantly lower concentrations of NO_2 (an O_3 precursor) on Saturdays (Figure 2-13). It also indicates MDA8 O_3 at those sites differs minimally between weekdays and weekends, with a maximum difference of 1.7~2.4 ppb. The data in this analysis are based on historic O_3 concentrations recorded between 2014 and 2019 (May–August).

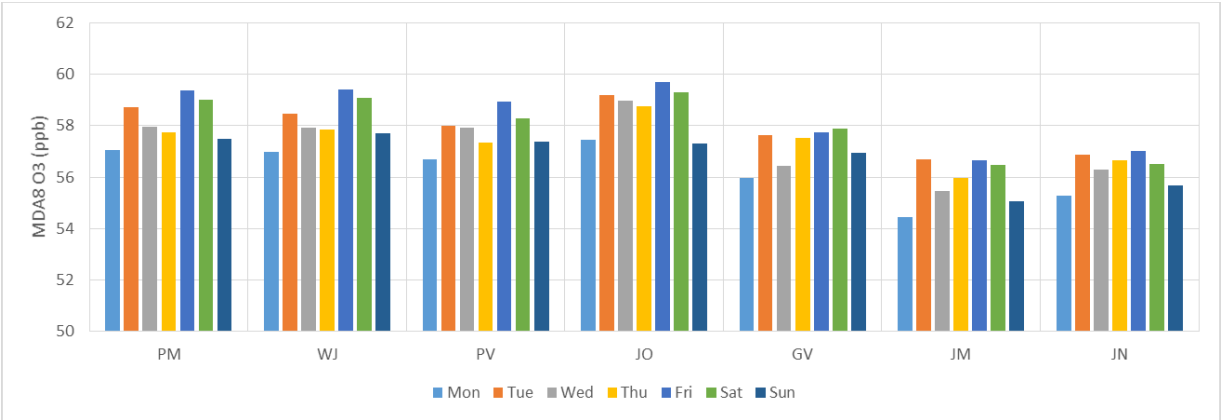

Figure 2-14. Weekly Pattern for MDA8 O_3 Average at Monitors, 2014–2019 (May–August).

3.0 EVENT SUMMARY AND CONCEPTUAL MODEL

3.1 PREVIOUS RESEARCH ON OZONE FORMATION AND SMOKE IMPACTS

The impact of wildfires on ozone concentrations at both local and regional levels has been studied extensively. Nikolov (2008) provides an excellent summary of past studies, as well as a conceptual discussion of the physical and chemical mechanisms contributing to observed impacts. Nikolov concludes that on a regional scale, biomass burning can significantly increase background surface ozone concentrations, resulting in NAAQS exceedances. Pfister et al. (2008) simulated the large fires of 2007 in northern and southern California; the authors found ozone increases of approximately 15 ppb in many locations and concluded, "Our findings demonstrate a clear impact of wildfires on surface ozone nearby and potentially far downwind from the fire location, and show that intense wildfire periods frequently can cause ozone levels to exceed current health standards." In a presentation at an emission inventory conference, Pace et al. (2007) modeled the June 2005 California fires, showing that the wildfire impacts added as much as 15 ppb to ozone concentrations in southern Nevada (Figure 3-1).

Finally, in one of DES's own studies (DES 2008), aircraft flights through smoke plumes demonstrated increased ozone concentrations of 15 to 30 ppb in California. Two other field campaign studies (DES 2013 & 2017) conducted by National Oceanic and Atmospheric Administration (NOAA) scientists have shown that large fires in California could have adversely impacted the air quality in Clark County.

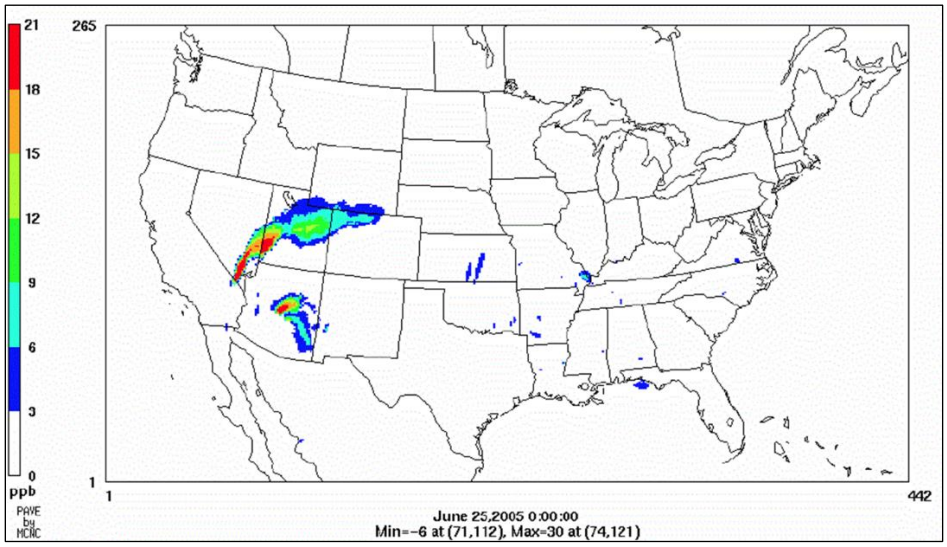

Figure 3-1. Difference ("Fire" / "No Fire") in Maximum 8-hour Ozone for June 25, 2005.

3.2 CALIFORNIA WILDFIRES IN 2018

Wildfires in the western states are worsening every year: they are bigger, hotter, more deadly, and more destructive. In California in 2018, the combination of natural fuel from a record 129 million trees killed by drought and bark beetles (as reported by the United States Forest Service) and compounding atmospheric conditions led to numerous large and small wildfires. The number

of fires and burned area increased greatly in June and July, as shown in Figure 3-2. Significant wildfires started breaking out in June of that year; later on in the summer, a series of large wildfires erupted across California, mostly in the northern part of the state, including the destructive Carr and Mendocino Complex Fires.

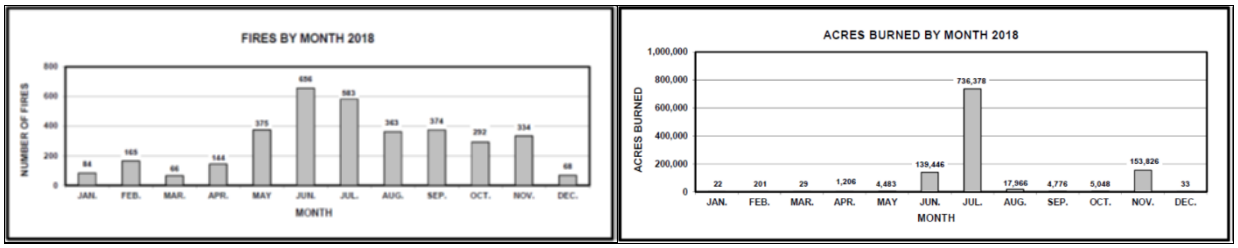

Source: CAL FIRE 2018 Wildfire Activity Statistics Report.

Figure 3-2. Number of Fires and Acres Burned by Month.

Figure 3-3 shows the more frequent ozone exceedances in the LVV after mid-June, reflecting the impact of the California wildfires during this period.

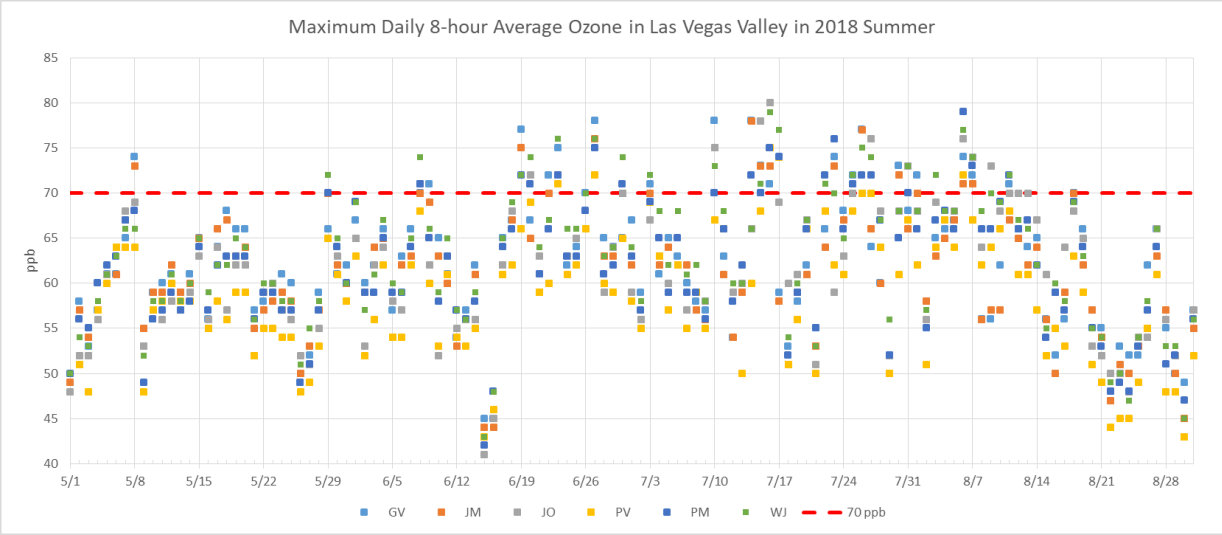

Figure 3-3. MDA8 Ozone Levels at LVV Monitors During 2018 Ozone Season.

3.3 JULY 25–27, 2018

In addition to the three ongoing large fires in California (Ferguson, Georges, and Lions) before the event day, another large fire (Cranston) broke out in southern California on July 25. By 6:00 a.m. on July 27, it had burned a total of 11,500 acres and was 3% contained, according to the InciWeb Incident Information System (https://web.archive.org/web/20181105230539/https://inciweb.nwcg.gov/incident/6032/).

The Ferguson Fire began the evening of July 13 when a catalytic converter ignited vegetation near Yosemite National Park; by the morning of July 27, the fire had burned a total of 45,911

acres and was 29% contained. The Georges Fire was started by lightning on the afternoon of July 8; by the morning of July 24, it had burned a total of 2,883 acres and was 70% contained. The Lions Fire was started by a lightning strike and first reported on June 11, 2018; by the afternoon of July 26, it had burned a total of 4,124 acres and was 85% contained. Figure 3-4 shows fire locations detected from the Moderate Resolution Imaging Spectroradiometer (MODIS) aboard the National Aeronautic and Space Administration (NASA) Aqua and Terra satellites and the Visible Infrared Imaging Radiometer Suite (VIIRS) aboard the Suomi National Polar-orbiting Partnership (Suomi-NPP) satellites on July 27; it also shows the smoke plumes transported to southern California/Nevada from different wildfires in central/southern California and the California/Mexico border area.

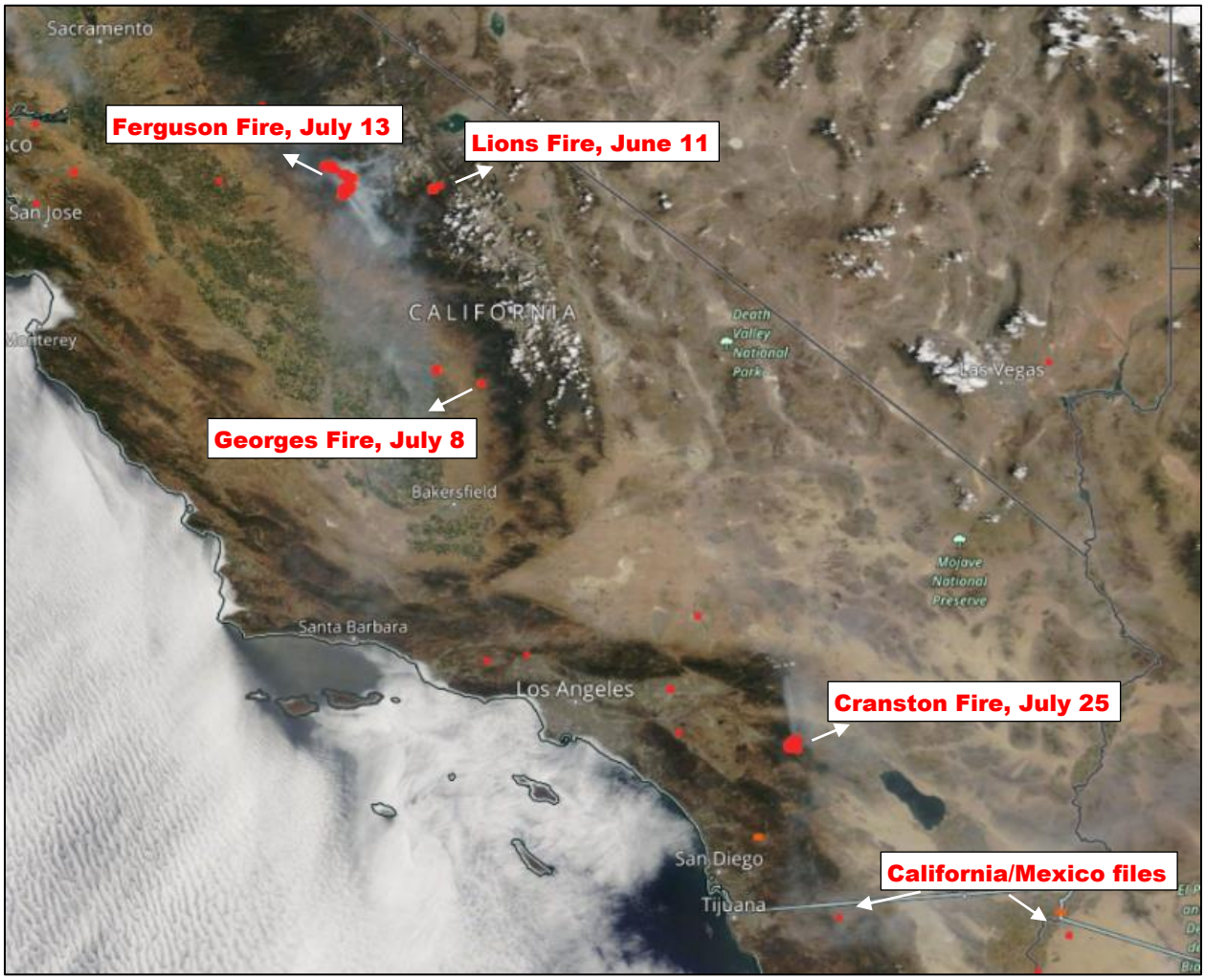

Source: NASA Worldview.

Figure 3-4. Fire Locations on July 27, 2018.

The 500-mb charts for July 24–27 in Figure 3-5 show that the synoptic weather pattern was dominated by a strong high pressure trough over the southwest U.S., resulting in stagnant weather over the LVV. Surface maps for July 24–27 (Figure 3-6) show surface thermal lows near Las Vegas, extending across California's Central Valley into northern California. A stationary front hovered over the area from Idaho through Utah to New Mexico; surface high pressure developed

between the stationary front and the trough extending to northern California. The airflows were mainly northwesterly from central California and southerly from southern California and the California/Mexico border area to the Mojave Desert and southern Nevada. Because winds associated with major high pressure systems are generally light, there is a greater chance for pollutants to accumulate in the atmospheric boundary layer. The skew-T diagrams in Figure 3-7 show July 25–27 had a strong temperature inversion and substantial stability, favoring ozone formation. These meteorological conditions, combined with the wildfire emissions transported from central/southern California and the Mexico border area, greatly increased levels of MDA8 O_3; Jerome Mack was at 77 ppb, the second highest value in 2018. Figure 3-8 illustrates a simplified conceptual model of the July 25-27, 2018, wildfire-influenced ozone event.

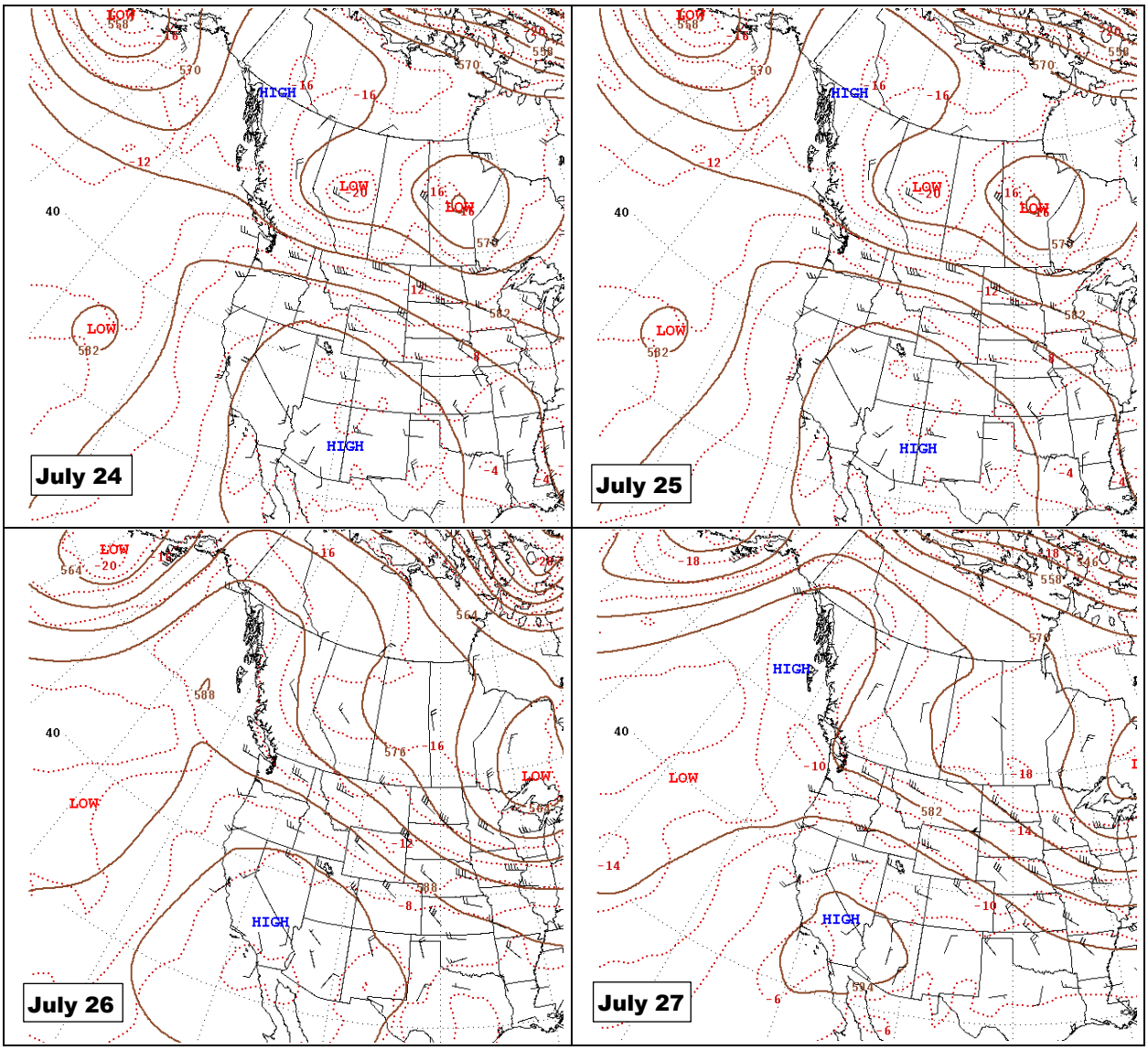

Source: NOAA, Weather Prediction Center

Figure 3-5. 500-mb Weather Patterns at 4 AM PST, July 24–27.

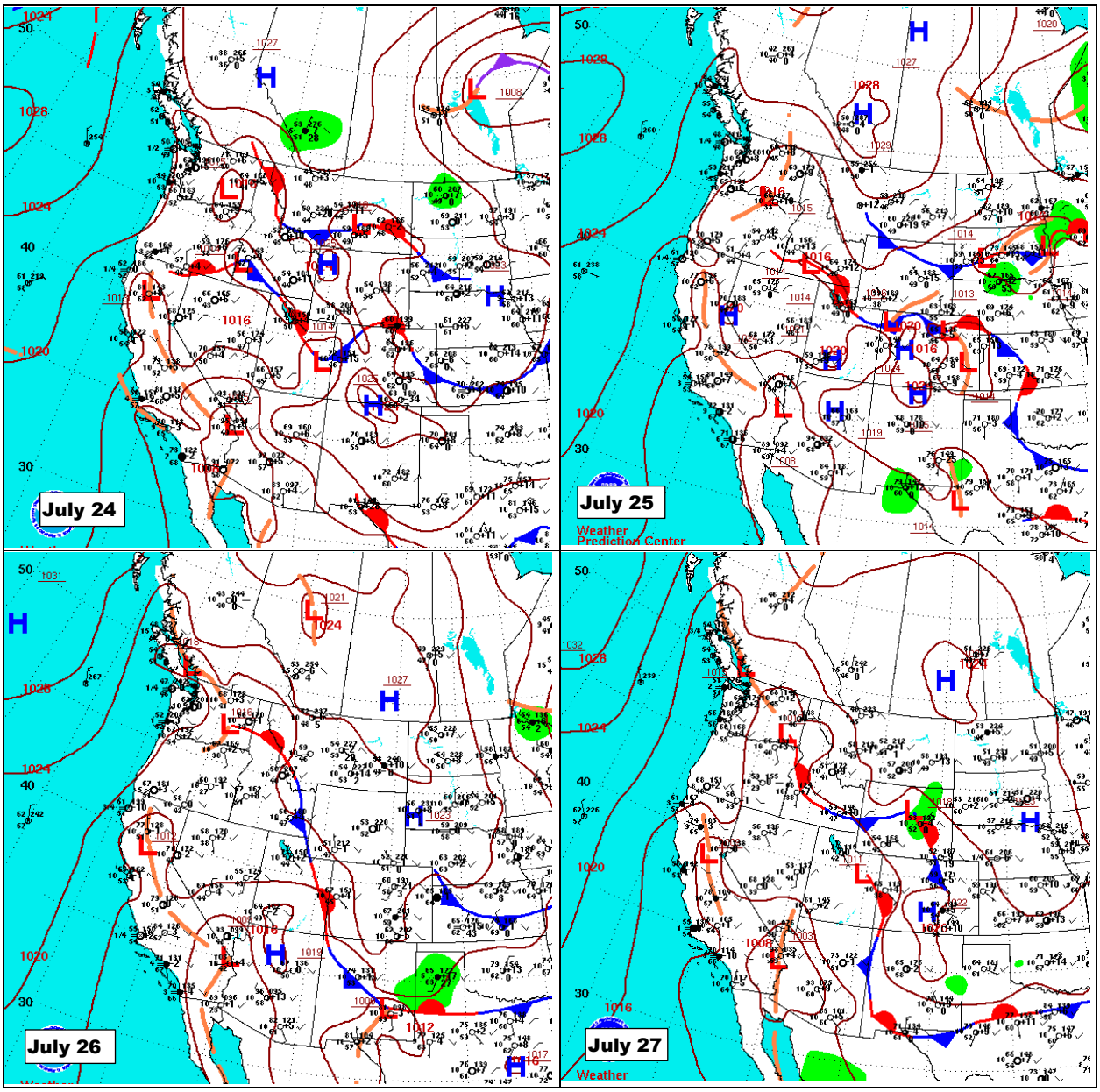

Source: NOAA, Weather Prediction Center

Figure 3-6. Surface Analysis for 4 AM PST, July 24–27.

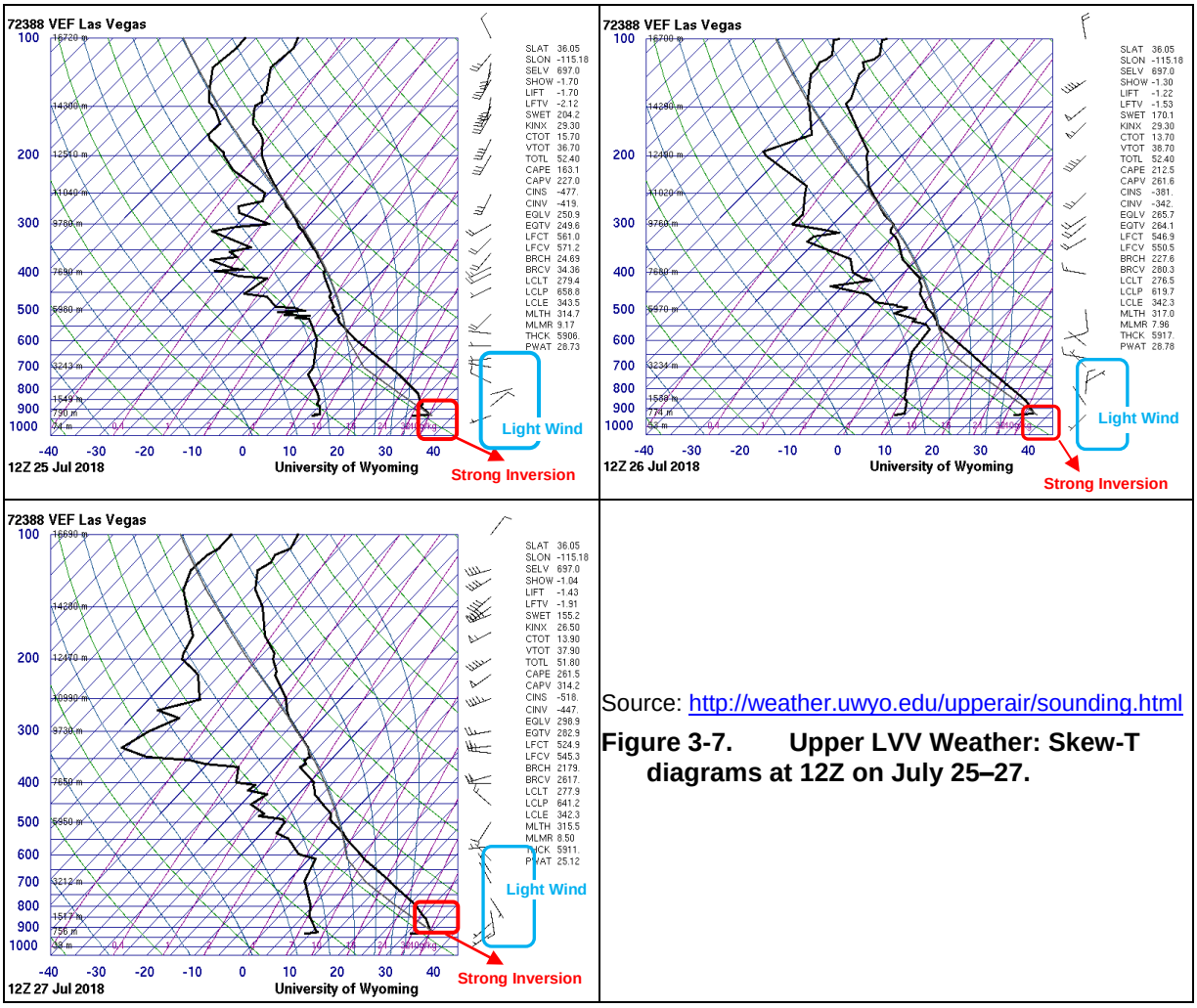

Source: http://weather.uwyo.edu/upperair/sounding.html

Figure 3-7. Upper LVV Weather: Skew-T diagrams at 12Z on July 25–27.

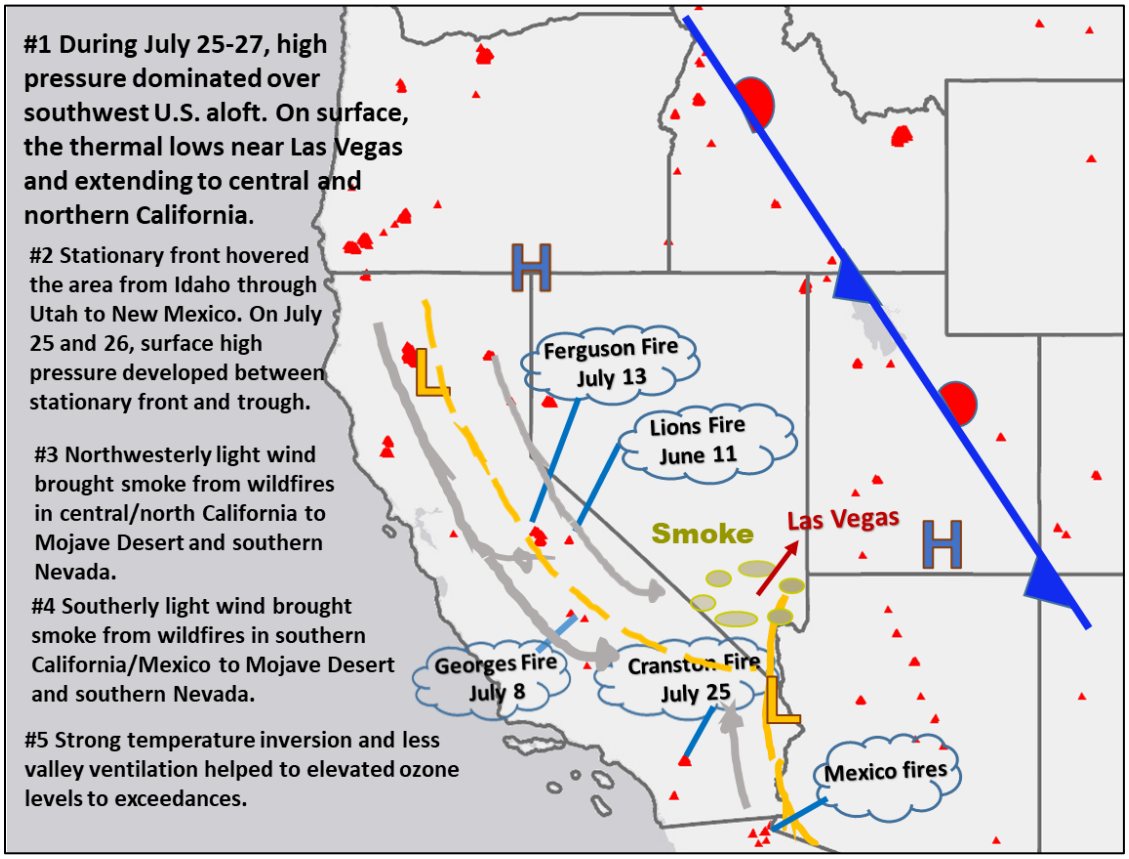

Figure 3-8. Simple Conceptual Model of July 25–27 Wildfire-Influenced Ozone Event.

4.0 CLEAR CAUSAL RELATIONSHIP

4.1 ANALYSIS APPROACH

Based on EPA's exceptional event guidance, this package provides Tier 1, Tier 2, and Tier 3 analyses to demonstrate a clear causal relationship between the wildfire event and monitored ozone exceedances. The demonstrations in this section provide (1) a comparison of the ozone data requested for exclusion against historical ozone concentrations at the monitor, and (2) a presentation of the path along which fire emissions were transported to the affected monitors.

Tier 1 Analyses

- Event day ozone concentrations are 5–10 ppb higher than non-event-related concentrations (95th percentiles for hourly seasonal ozone for 2014–2018).

Tier 2 Analyses

- Key Factor #1: Q/d Analysis (not performed).
- Key Factor #2: Comparison of the event-related MDA8 ozone with historical non-event-related high ozone concentrations (>99th percentile from 2014 to 2018 of MDA8 ozone, or the top four highest daily ozone measurements).
- Visible satellite imagery.
- Hazard Mapping System (HMS) smoke map.
- Hybrid Single-Particle Lagrangian Integrated Trajectory (HYSPLIT) model backward trajectories.
- Cloud-Aerosol Lidar and Infrared Pathfinder Satellite Observation (CALIPSO) satellite retrieval: Vertical profile measurements of atmospheric aerosols.
- Concurrent rise in ozone concentrations.
- Analysis of $PM_{2.5}$ speciation data.
- Analysis of levoglucosan (trace of fire emissions).
- Supporting ground measurements: Event-related diurnal $PM_{2.5}$, NO_2, and CO (i.e., wildfire plume components) concentrations showed elevated concentrations and/or changes in diurnal profile consistent with smoke impacts.

Tier 3 Analyses

- GAM statistical model.

Key factor #1 for a Tier 2 analysis uses an **emissions divided by distance (Q/d)** relationship to estimate the influence of fire emissions on a downwind monitor. If Q/d • (daily aggregated fires) ≥ 100, then the fires satisfy the Q/d test. A Q/d analysis for August 6, the day with the highest smoke impact in 2018, was performed in the concurrent *Exceptional Event Demonstration for Ozone Exceedances in Clark County, Nevada—August 6-7, 2020*. Even using the smoke from all three large wildfires in 2018 and other small wildfires in California during the August 6–7, 2018 event, the Q/d threshold could not be achieved due to the significant distance between Las Vegas

and the wildfires' origin points. Therefore, this document provides no Q/d analyses for this event.

In addition to analysis of $PM_{2.5}$ speciation data, levoglucosan—a unique tracer for burning biomass in $PM_{2.5}$ samples—can serve as a wildfire indicator. Levoglucosan has an atmospheric lifetime of one to four days before it is lost due to atmospheric oxidation, and can therefore be used as a tracer of biomass burning (wildfires) far downwind from its source (Hoffmann et al. 2009; Hennigan et al. 2010; Bhattarai et al. 2019; Lai et al. 2014). During the summer of 2018, DES collected $PM_{2.5}$ samples every three days at the Jerome Mack and Sunrise Acres monitoring stations. Sample analysis—including for levoglucosan, a wildfire marker—was done by the Desert Research Institute (DRI).

A GAM is a type of statistical model that allows the user to predict a response based on the linear and non-linear effects of multiple variables (Wood 2017). A GAM model developed by Sonoma Technology was used to describe the relationship between MDA8 ozone levels and primary predictors (e.g., prior day's ozone, meteorology, and transport) from 2014–2020. The details for the model's construction and verification are described in Section 3.3.3, "GAM Statistical Modeling," of *Exceptional Event Demonstration for Ozone Exceedances in Clark County, Nevada—June 22, 2020*. By comparing GAM-predicted ozone values with actual measured ozone concentrations (i.e., residuals), we can determine the effect of outside influences (e.g., wildfires or stratospheric intrusions) on ozone concentrations each day (Jaffe et al. 2004). The GAM model results presented in this document contain MDA8 ozone predictions, residuals, positive 95th percentile value, predicted fire influence, and percentile rank of positive residuals based on EPA guidance (EPA 2016), which were used to estimate wildfire influence under the meteorological conditions recorded at exceeding sites.

4.2 COMPARISON OF EVENT-RELATED CONCENTRATIONS WITH HISTORICAL CONCENTRATIONS

Outside the transport of ozone and its precursors from California wildfires, elevated ozone levels in the LVV correlate to local weather conditions and home-grown (Figure 2-7) and upwind (Figure 2-8) California emissions. The declining ozone trend in the LVV (Figure 2-9) reflects the reduction of these emissions over the years. However, 2018 was an exceptional year, with more ozone exceedances than any of the prior years of 2014–2017 (Figure 1-1).

In general, warm, dry weather is more conducive to ozone formation than cool, wet weather. High winds tend to disperse pollutants and can dilute ozone concentrations. We examined three meteorological variables—daily maximum surface temperature, daily average wind speed, and daily average relative humidity—at McCarran International Airport during the 2014–2018 summer months to depict the year-to-year variation of local weather conditions (Figure 4-1).

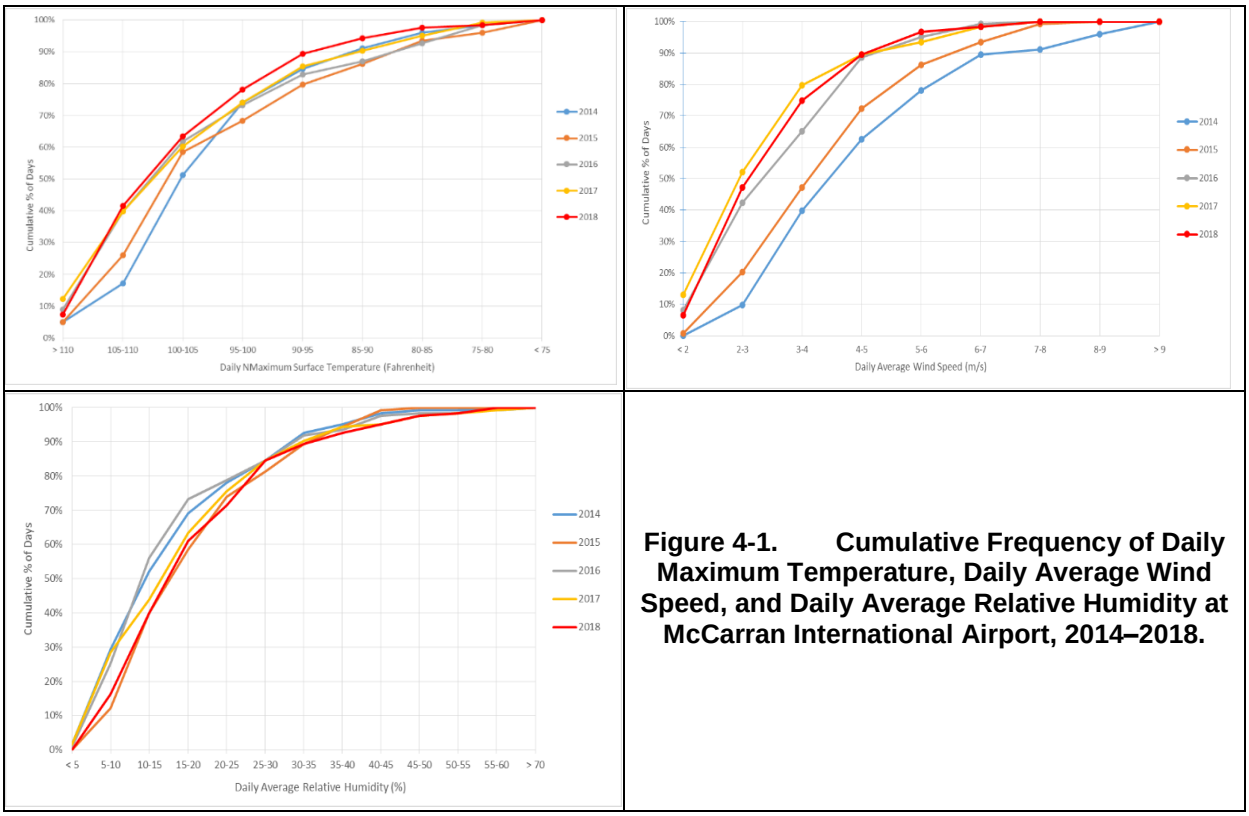

Figure 4-1. Cumulative Frequency of Daily Maximum Temperature, Daily Average Wind Speed, and Daily Average Relative Humidity at McCarran International Airport, 2014–2018.

Overall, 2018 had lower wind speeds, slightly higher temperatures, and slightly more moisture compared to previous years. Yet the mean of 2018 MDA8 ozone is between 4.4 and 7.2 ppb higher than other years (Figure 4-2). Compared to 2014–2017, summer 2018 had more California wildfires (Figure 1-1) and relatively stagnant weather conditions (Figure 4-1). This increased the background ozone levels in the LVV (Figure 4-2), resulting in a higher number of ozone exceedances than in previous years.

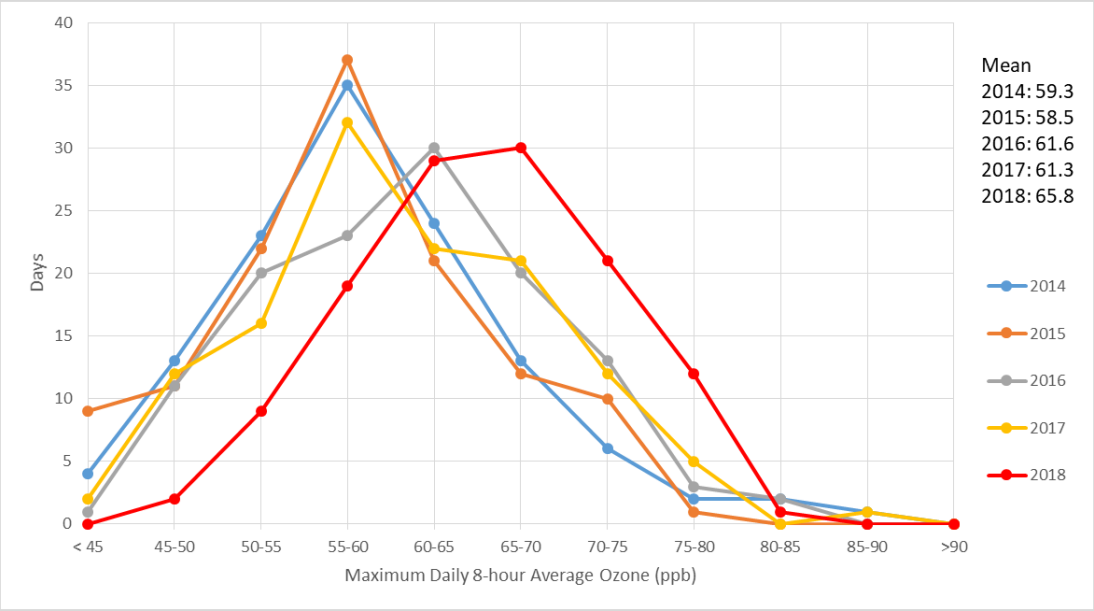

Figure 4-2. Distribution of Days by MDA8 Ozone Levels, 2014–2018.

Figures 4-3 through 4-8 show MDA8 ozone during the 2014–2018 ozone seasons plotted for each monitor against that monitor's multiseason 95th and 99th percentiles. Red circles indicate the ozone exceedances submitted for the 2018 exceptional events demonstration. All but the following sites and dates exceeded the 95th percentile: Walter Johnson on June 19 and July 15; Palo Verde on July 26 and 27; and Joe Neal on June 20, 23, and 27.

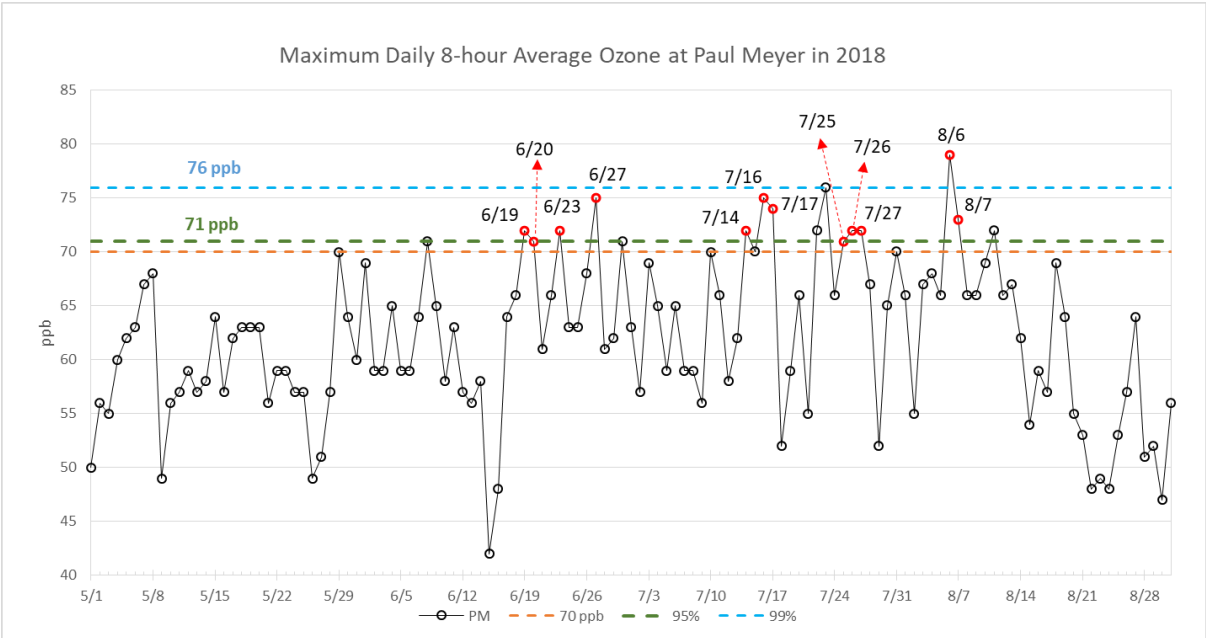

Figure 4-3. MDA8 Ozone at Paul Meyer, 2018 Ozone Season.

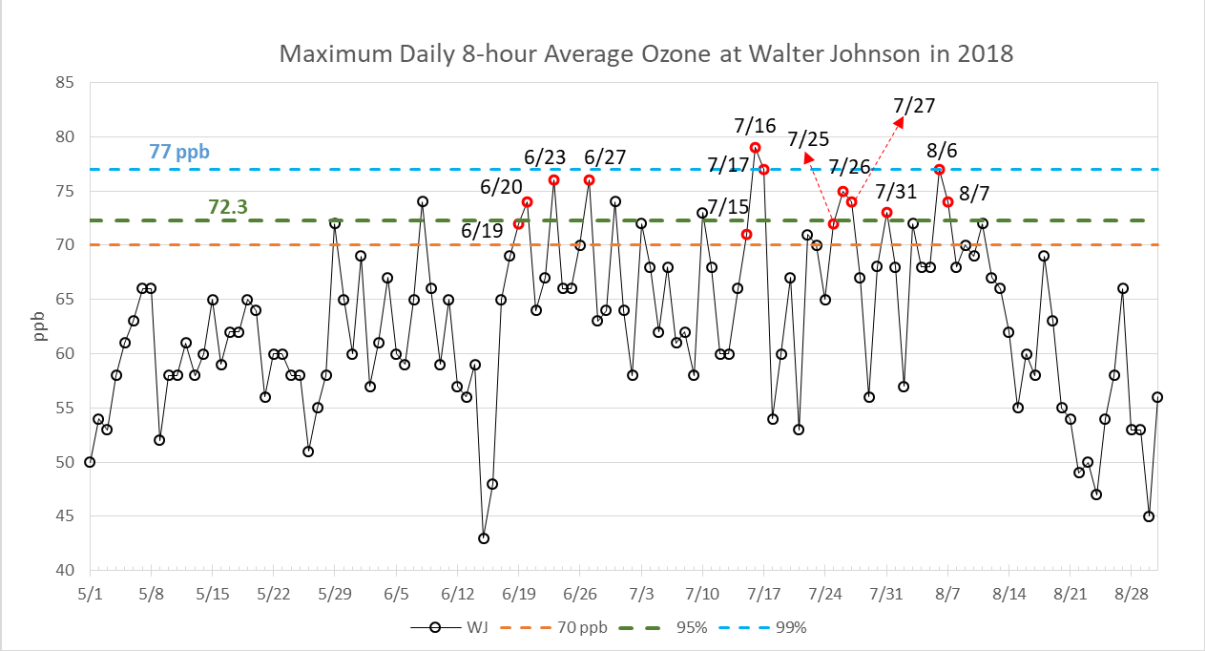

Figure 4-4. MDA8 Ozone at Walter Johnson, 2018 Ozone Season.

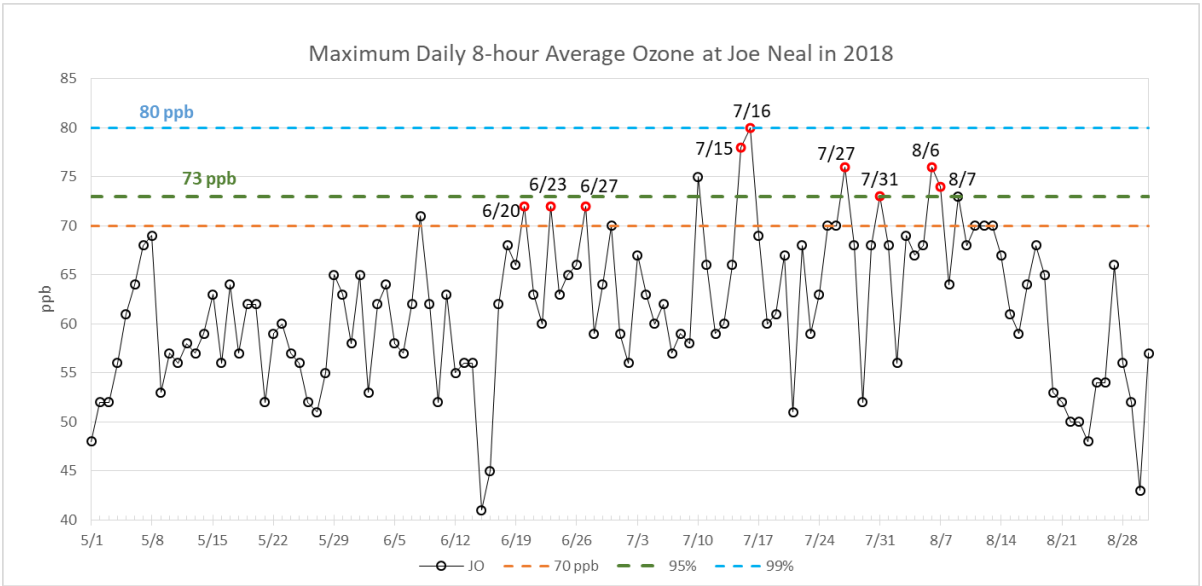

Figure 4-5. MDA8 Ozone at Joe Neal, 2018 Ozone Season.

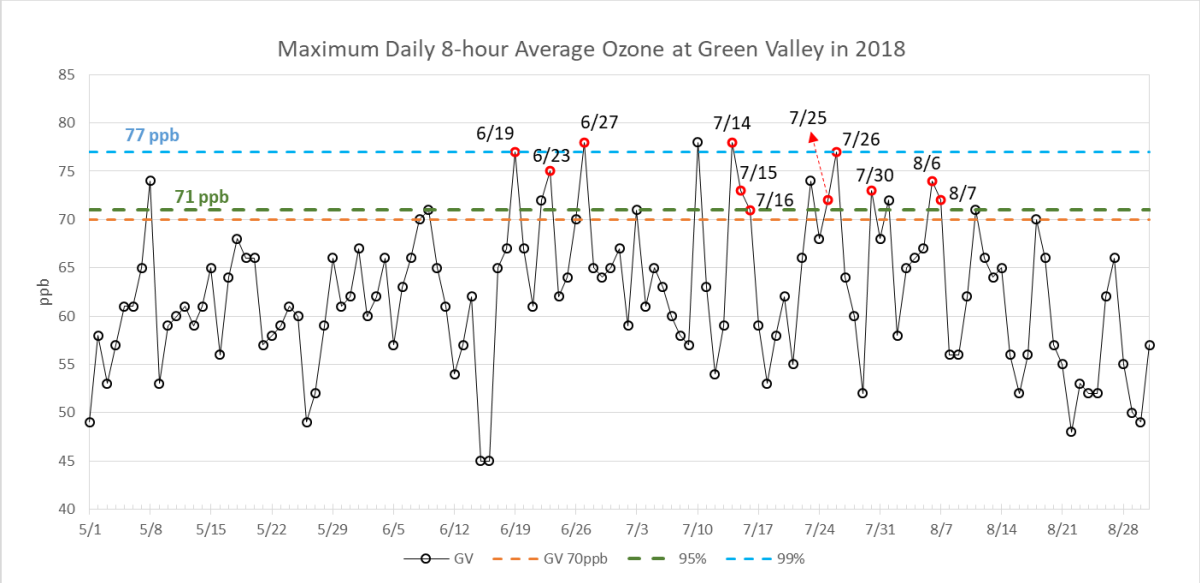

Figure 4-6. MDA8 Ozone at Green Valley, 2018 Ozone Season.

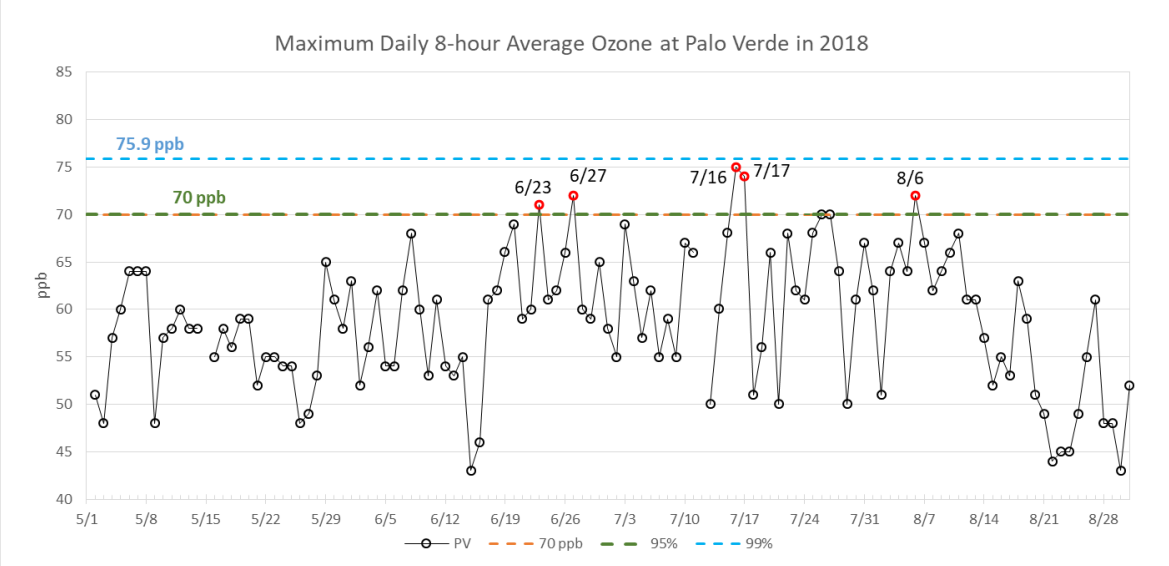

Figure 4-7. MDA8 Ozone at Palo Verde, 2018 Ozone Season.

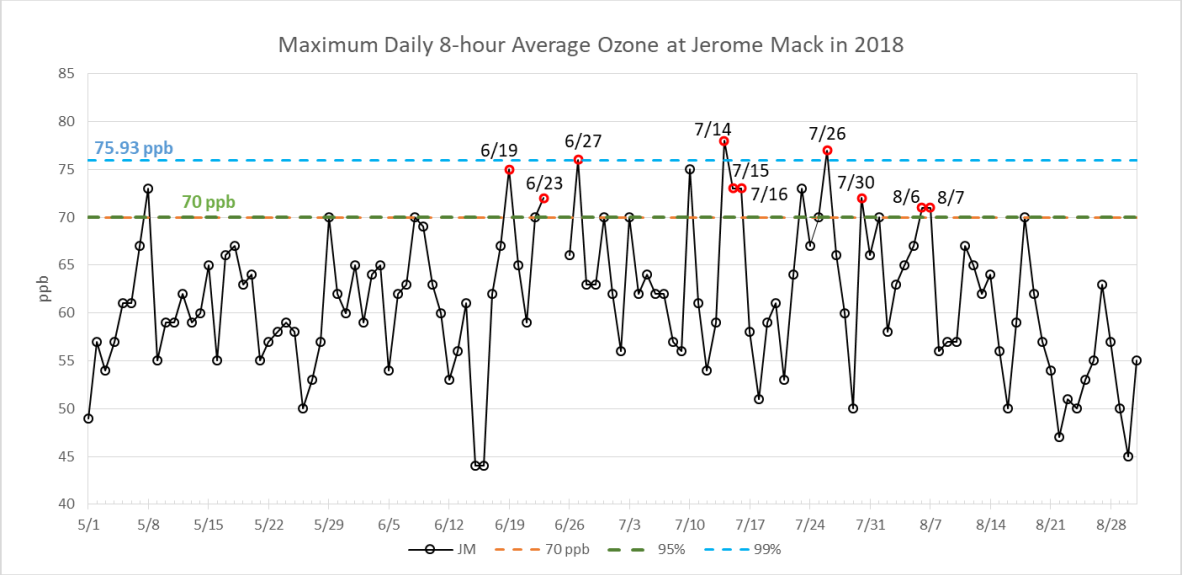

Figure 4-8. MDA8 Ozone at Jerome Mack, 2018 Ozone Season.

The ratio of $PM_{2.5}$ organic carbon (OC) to elemental carbon (EC) has been used to differentiate combustion sources of biomass burning and mobile sources, since biomass burning usually has a higher OC/EC ratio (ranging between 7 and 15) (Lee et al. 2005; Pio et al. 2008) than gasoline (ranging between 3.0 and 4.0) or diesel vehicles (<1.0) (Lee and Russell 2007; Zheng et al. 2007). The acquired $PM_{2.5}$ of OC and EC from EPA's Air Quality System (https://aqs.epa.gov/aqsweb/airdata/download_files.html) is available only for Jerome Mack in the LVV on a three-day sampling schedule.

Figure 4-9 shows the OC/EC ratio for May–August in 2018 and 2019 against the median OC/EC ratio for May–August (5.4, orange line) and September–April (3.4, green line) according to 2015–2017 and 2019 data. It clearly shows a larger wildfire influence in ozone season months than non-ozone season months, and more days impacted by wildfire during ozone season months in 2018 than 2019 (a clean year with the annual 4th highest MDA8 ozone for all monitors below the 2015 ozone NAAQS). Figure 4-10 shows a similar OC/EC ratio plot for an upwind monitor located at Rubidoux in the Riverside-San Bernardino, CA, area with the median value for May–August (6.8, orange line) and September–April (3.4, green line). Comparing Figures 4-9 and 4-10 shows the daily variation in the OC/EC ratio at Jerome Mack generally follows the variation at Rubidoux, and that more days in 2018 than 2019 had an OC/EC ratio above the median value for both monitors. It strongly indicates Jerome Mack was frequently impacted by California wildfires in 2018.

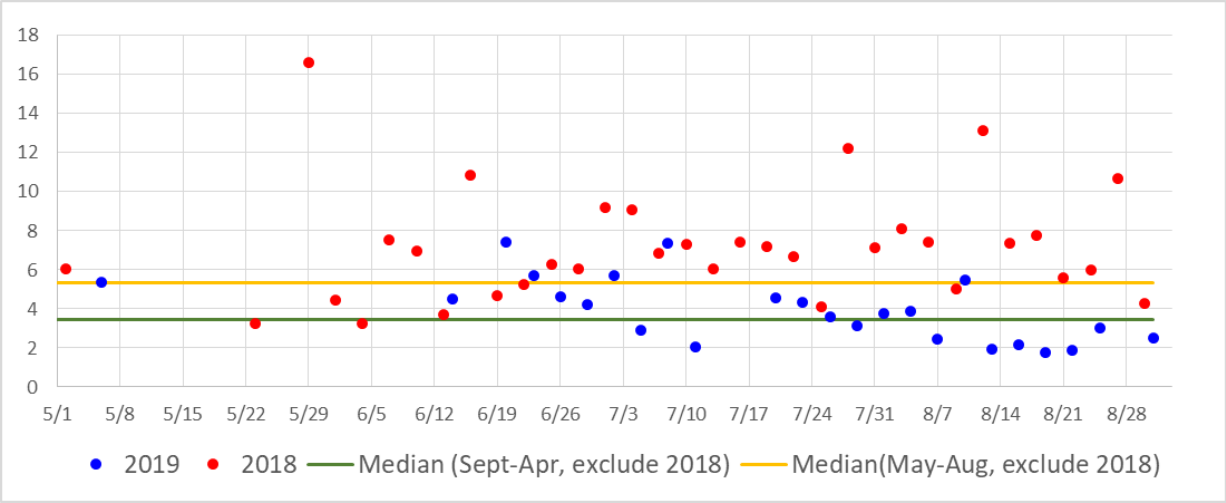

Figure 4-9. OC/EC ratio at Jerome Mack, 2018-2019 Ozone Season.

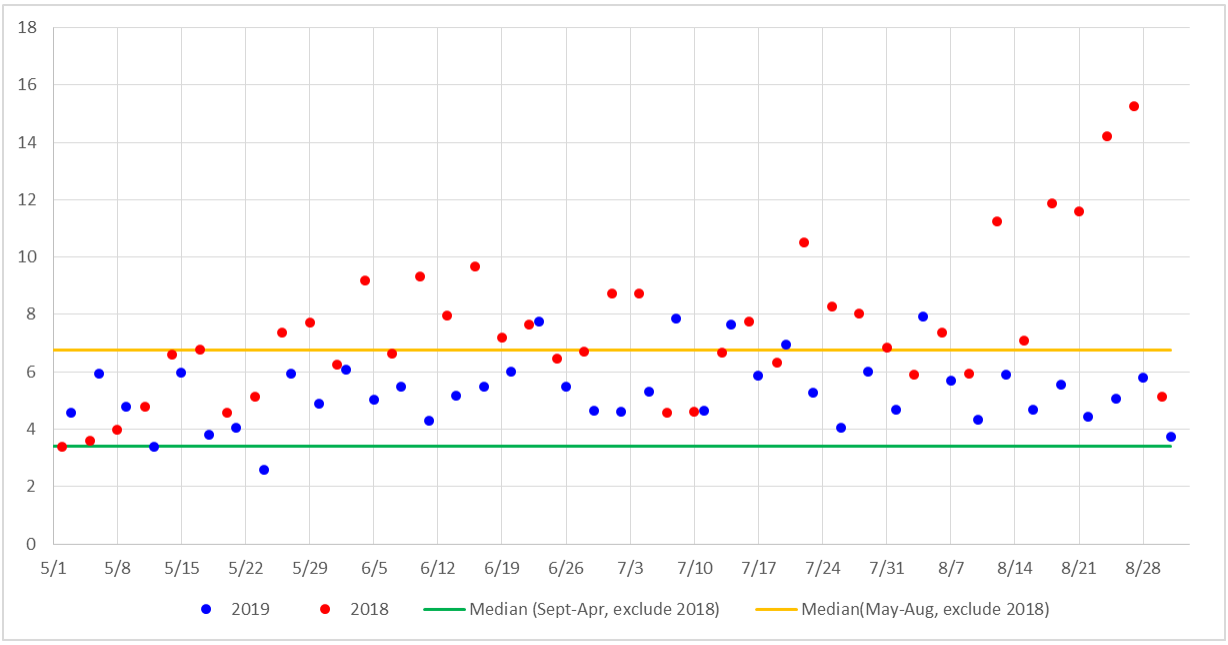

Figure 4-10. OC/EC ratio at Rubidoux, CA, 2018-2019 Ozone Season.

4.3 EVENT OF JULY 25–27, 2018

4.3.1 Tier 1 Analysis: Historical Concentrations

Figures 4-11 and 4-12 show the hourly seasonal percentiles for ozone from 2014–2018 compared to measured hourly ozone on July 25–27, 2018, at exceeding sites.

- On July 25, the increases in O_3 at Paul Meyer, Walter Johnson, and Green Valley were 12, 12, and 6 ppb, respectively.

- On July 26, the increases in O_3 at Paul Meyer, Walter Johnson, Green Valley, and Jerome Mack were 4, 11, 13, and 11 ppb, respectively.

- On July 27, the increases in O_3 at Paul Meyer, Walter Johnson, and Joe Neal were 5, 7, and 10 ppb, respectively.

Not all exceeding monitors on July 25–27 were 5–10 ppb higher than non-event-related concentrations, nor did they occur outside the area's normal high-ozone season. Thus, Tier 2 analyses were performed to provide additional evidence of the clear causal relationship between wildfire emissions and ozone exceedances. Although a few exceeding monitors were at or below the threshold of 5 ppb higher than non-event-related concentrations, many of the exceedances were more than 10 ppb higher and provide evidence that an extreme event occurred.

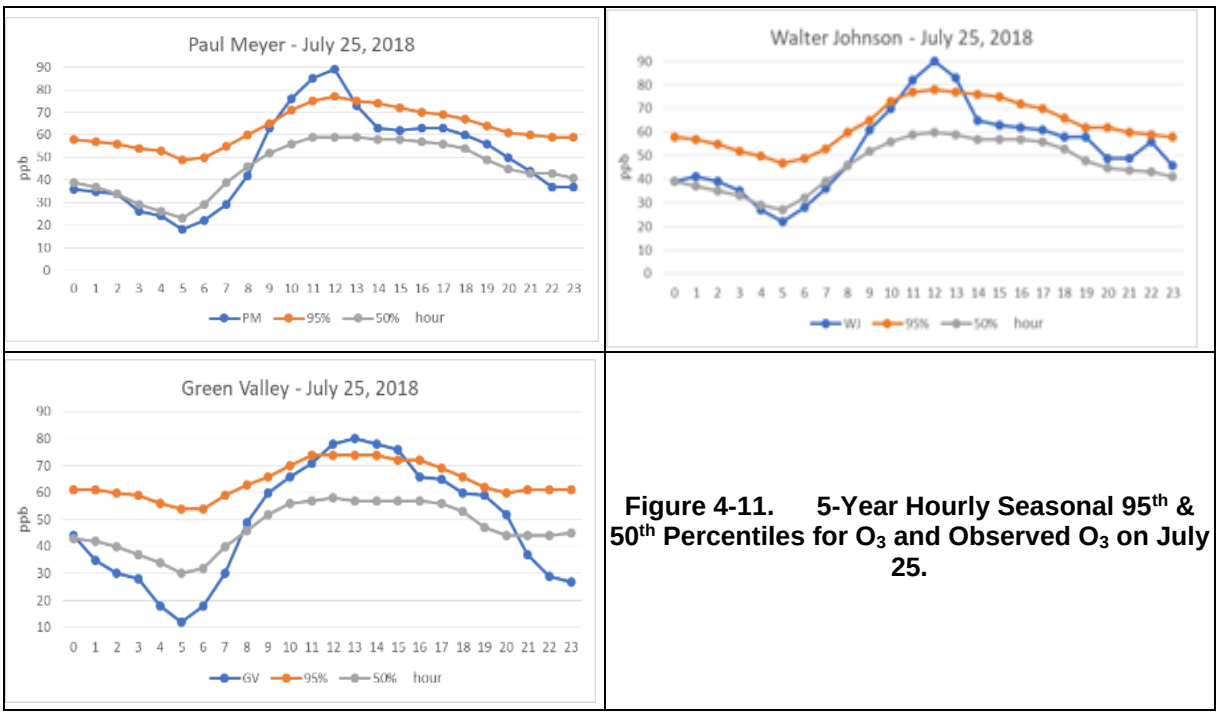

Figure 4-11. 5-Year Hourly Seasonal 95th & 50th Percentiles for O_3 and Observed O_3 on July 25.

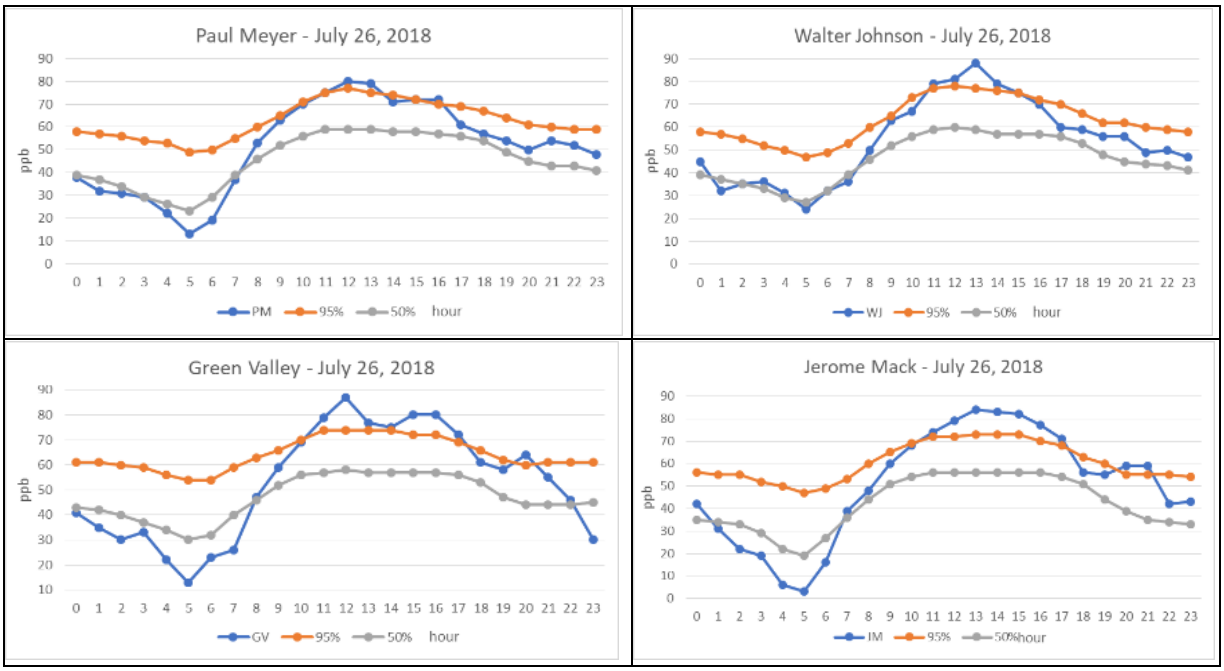

Figure 4-12. 5-Year Hourly Seasonal 95th & 50th Percentiles for O_3 and Observed O_3 on July 26.

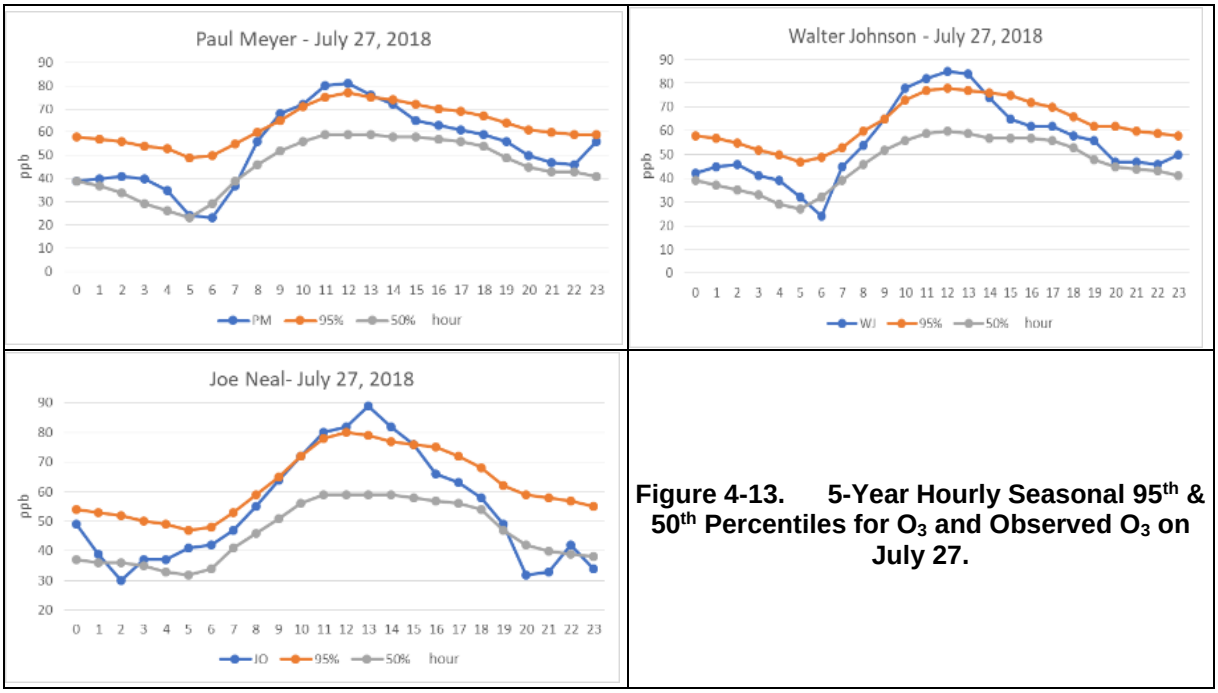

Figure 4-13. 5-Year Hourly Seasonal 95th & 50th Percentiles for O_3 and Observed O_3 on July 27.

4.3.2 Tier 2 Analysis

4.3.2.1 Key Factor #2

Figures 4-3, 4-4, and 4-6 compare historical non-event ozone season concentrations at Paul Meyer, Walter Johnson, and Green Valley to the July 25–27 event. Only the July 26 O_3 exceedances at Green Valley and Jerome Mack are higher than the five-year 99th percentile value. However, each day during this event has three to four sites where O_3 levels exceeded the five-year 95th percentile value, depending on local airflow direction. Additionally, O_3 exceedances on July 26 at Green Valley and Jerome Mack were ranked the fourth and second highest values in 2018 (Table 1-1). The ozone exceedance on July 27 at Joe Neal is ranked as one of the fourth highest values in 2018 (Table 1-1). The Key Factor #2 analysis results thus do not meet the criteria to support a demonstration that ozone exceedances on July 25–27 were caused by an exceptional event; however, they are evidence of the presence of an extreme event.

4.3.2.2 Evidence of Fire Emissions Transport to Area Monitors

Visible Satellite Imagery

Visible satellite imagery from NASA's MODIS (Aqua/Terra) and VIIRS/Suomi-NPP show transport of smoke from wildfires in California and Mexico to the southwestern U.S., including the LVV, on July 25–27 (Figures 4-14, 4-15, and 3-4). During these days, continuous smoke from wildfires was transported either southwestward or northward, depending on airflow, as depicted in Figure 3-8 (the conceptual model). Therefore, wildfire emission dominated the air in southern California and Nevada.

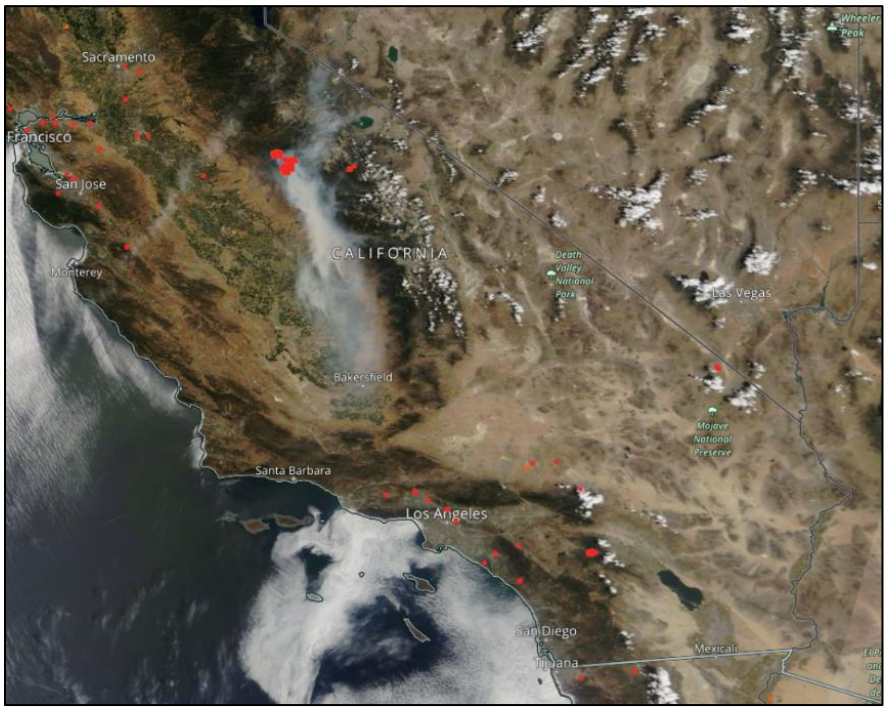

Source: NASA Worldview.

Figure 4-14. Visible Satellite Imagery, July 25.

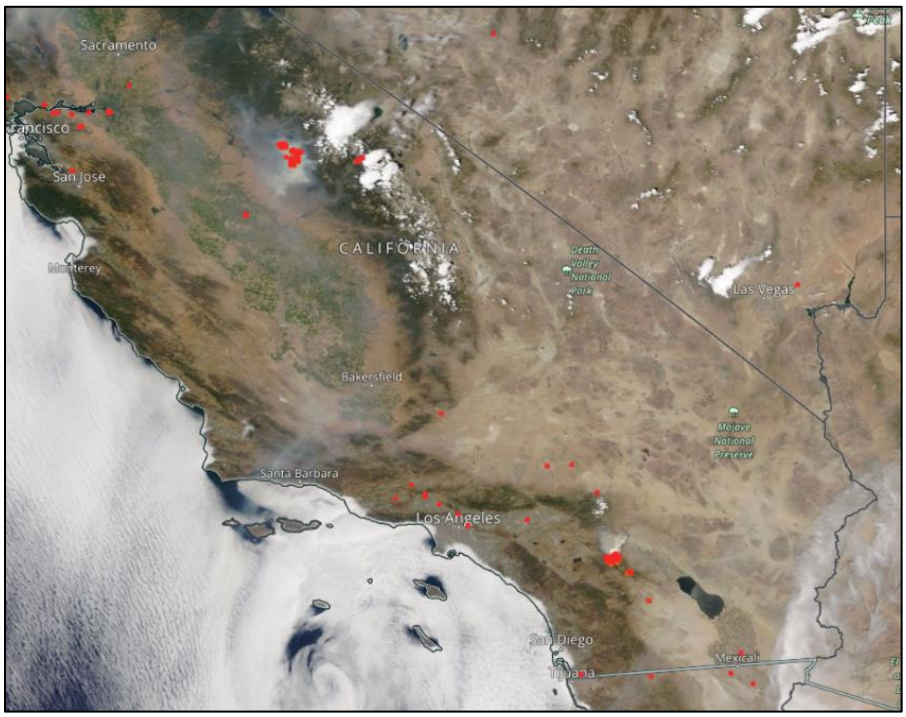

Source: NASA Worldview.

Figure 4-15. Visible Satellite Imagery, July 26.

NOAA Daily HMS Smoke Map Superimposed on HYSPLIT Backward Trajectories

The HMS can demonstrate the transport of fire emissions to impacted monitors. Examining HMS smoke analyses together with HYSPLIT backward trajectories provides stronger evidence of wildfire emissions being transported to the monitoring sites.

The HYSPLIT model was run to produce back trajectories of air parcel movement at 10, 100, and 1,000 m (EPA guidance recommends within 100~1,500) for exceeding monitors. Figures 4-15 through 4-17 show daily HMS smoke maps superimposed on 24-hour backward trajectories of airflows arriving at the selected monitors at 1:00 p.m. on July 25, 26, and 27. The smoke plume is evident across California and Nevada, and wind speeds were demonstrably low in the LVV during this period. Both conditions elevated ozone levels above 70 ppb; therefore, the trajectories demonstrate that smoke was transported from California and the Mexico border to the LVV.

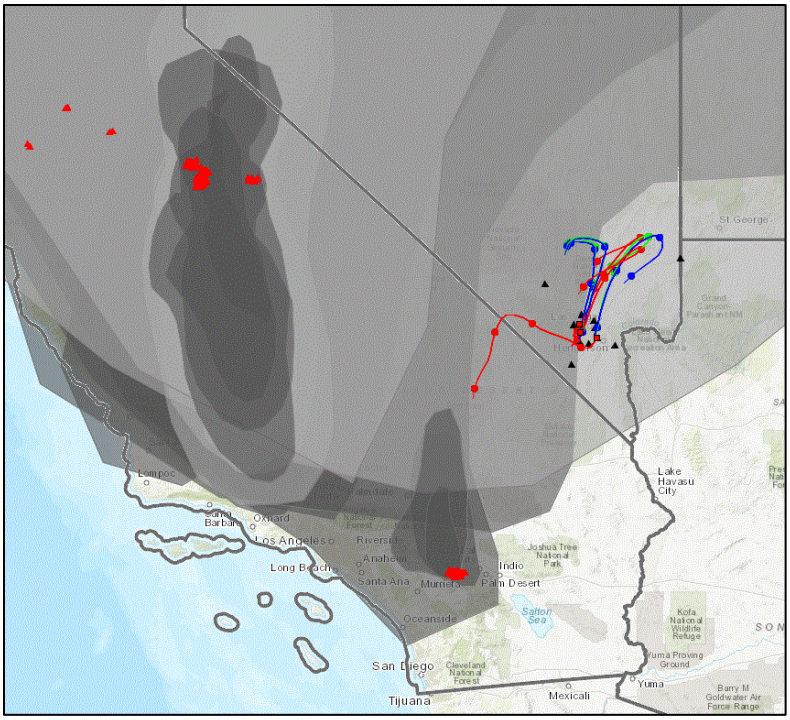

Note: Red = 1000 m, blue = 100 m, green = 10 m.

Figure 4-16. 24-hr Backward Trajectories at GV, WJ, and PM as of 1 PM PST on July 25.

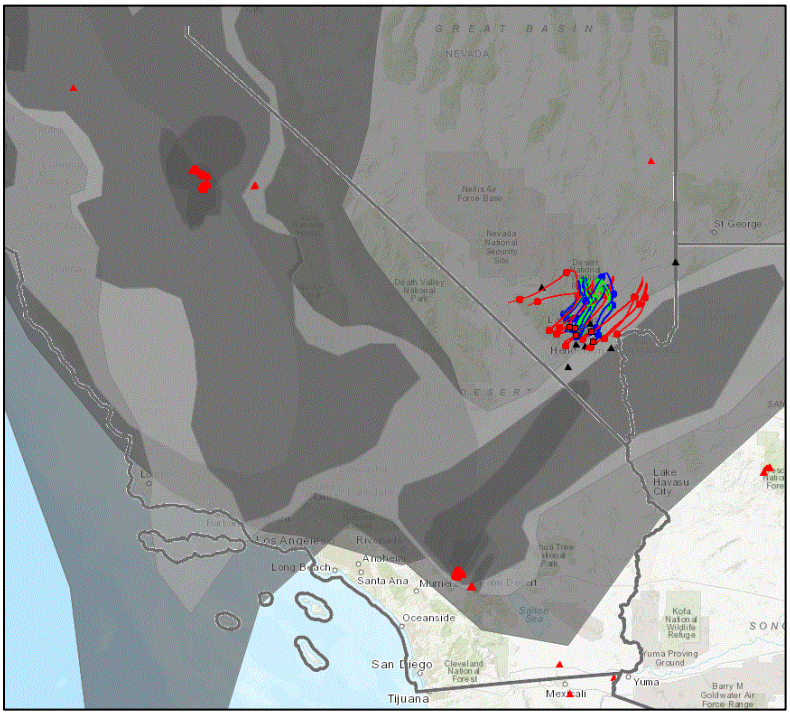

Note: Red = 1000 m, blue = 100 m, green = 10 m.

Figure 4-17. 24-hr Backward Trajectories at GV, JM, WJ, PM, and PV as of 1 PM PST on July 26.

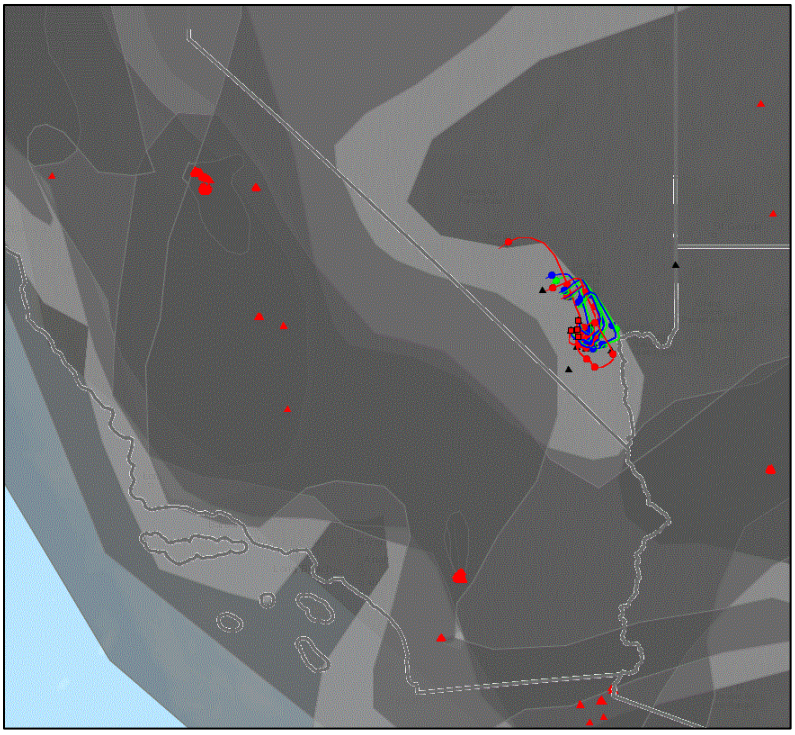

Note: Red = 1000 m, blue = 100 m, green = 10 m.

Figure 4-18. 24-hr Backward Trajectories at JO, WJ, PM, and PV as of 1 PM PST on July 27.

Satellite Retrieval—CALIPSO

We also examined data retrieved from the CALIPSO satellite, launched in June 2006. To make use of this data, we identified the vertical profile of atmospheric aerosols. The best CALIPSO aerosol retrieval over LVV during this time was around 1:30 p.m. PST on July 25. An examination of CALIPSO's orbital track over the southwest U.S. and the vertical profile of corresponding aerosols (Figures 4-18 and 4-19) allowed us to categorize the aerosol types over southern Nevada as polluted continental/smoke, slight elevated smoke, and large polluted dust.

The aerosol type of "polluted dust" is assigned a lidar ratio of 55+22 sr in the CALIPSO V3 and V4 algorithms (Kim et al. 2018). Based on research conducted by Burton et al. (2013), we compared CALIPSO V3 aerosol classifications with measurements made by NASA from the airborne High Spectral Resolution Lidar (HSRL). The results showed poor agreement for smoke (13%) or polluted dust (35%). In particular, the polluted-dust type is overused due to an attenuation-related depolarization bias. Burton found CALIPSO's identification of internal boundaries between different aerosol types in contact with one another frequently do not reflect actual transitions between aerosol types accurately; therefore, it is reasonable to suspect the large area of polluted dust could be smoke.

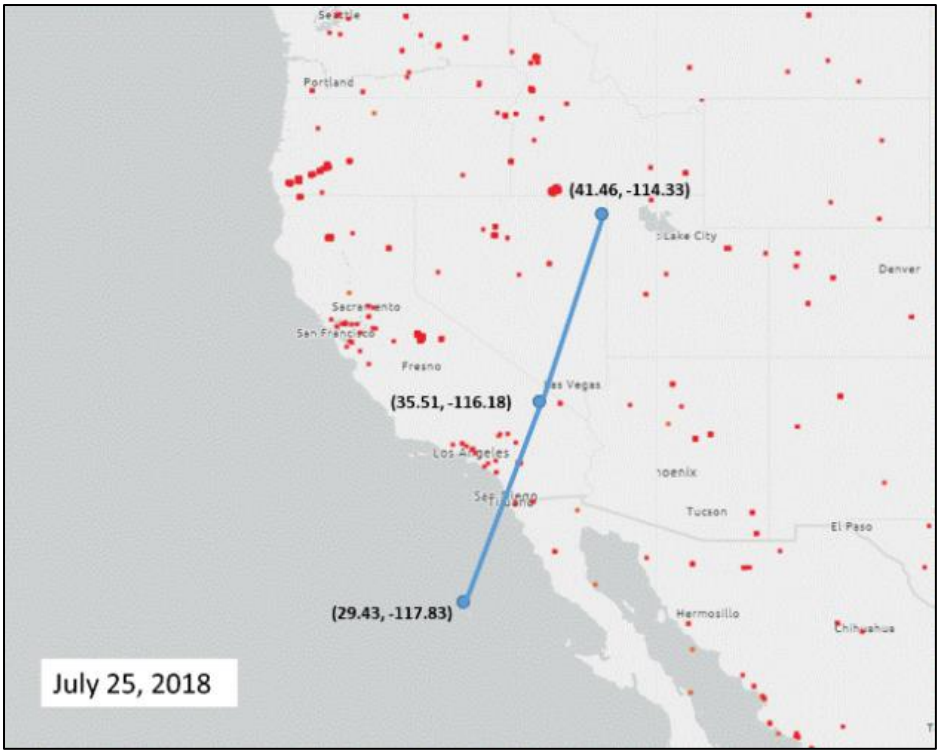

Figure 4-19. CALIPSO Orbital Track over Southwest U.S. on July 25.

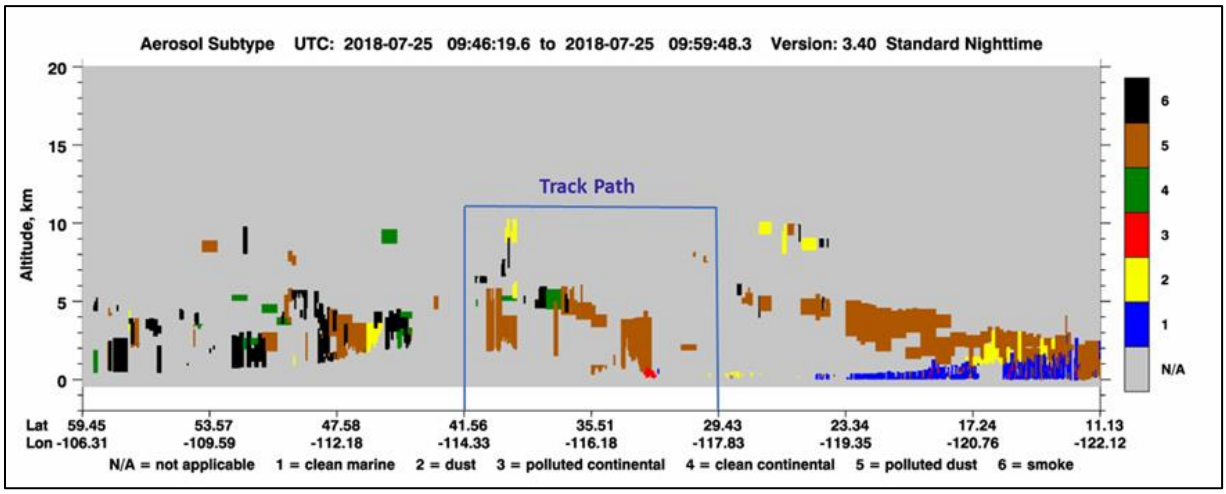

Note: The upper air near the LVV is circled in blue.

Figure 4-20. CALIPSO Aerosol Type Vertical Profile Collected on July 25.

4.3.2.3 Evidence that Fire Emissions Affected Area Monitors

Concurrent Rise in Ozone Concentrations

We examined MDA8 O_3 levels at monitors inside (Figure 2-2) and outside (Figure 4-20) the LVV on July 24–28, 2018. Visible satellite imagery, HMS smoke analysis, backward trajectories, satellite retrievals, and the meteorological conditions detailed in Section 3.3 depict the

transport of smoke, ozone, and ozone precursor emissions from wildfires in central/southern California and on the Mexico border to the LVV. The widespread smoke on July 24–27 (Figure 4-21) appears to have had a significant influence on ozone concentrations, with MDA8 O_3 above the 50th and near/above the 95th percentile value during this period at Mojave, Jean, and Mesquite. Similarly, widespread smoke added to local emissions, along with meteorological conditions favoring ozone formation, elevated MDA8 O_3 near/above the 95th percentile value at monitors in the LVV (Figure 4-22).

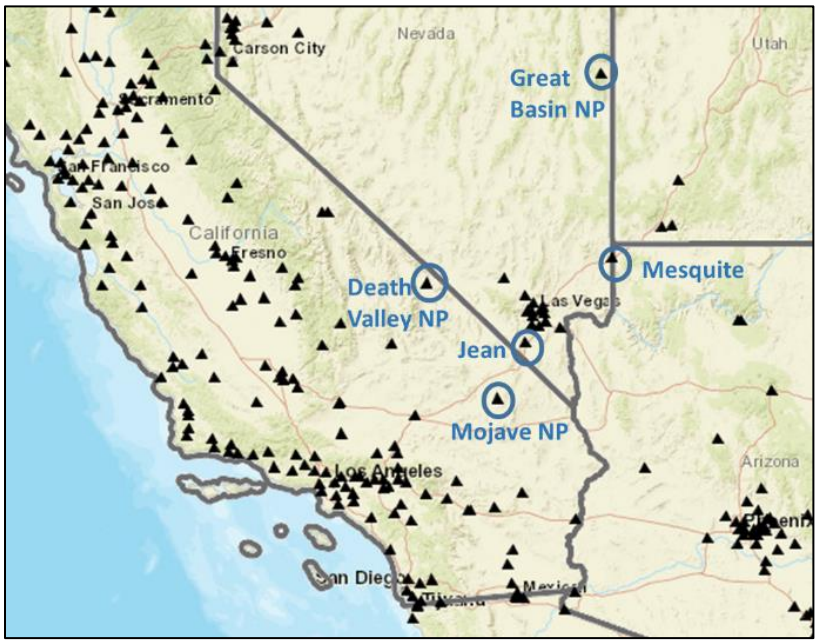

Figure 4-21. Monitors Outside the LVV.

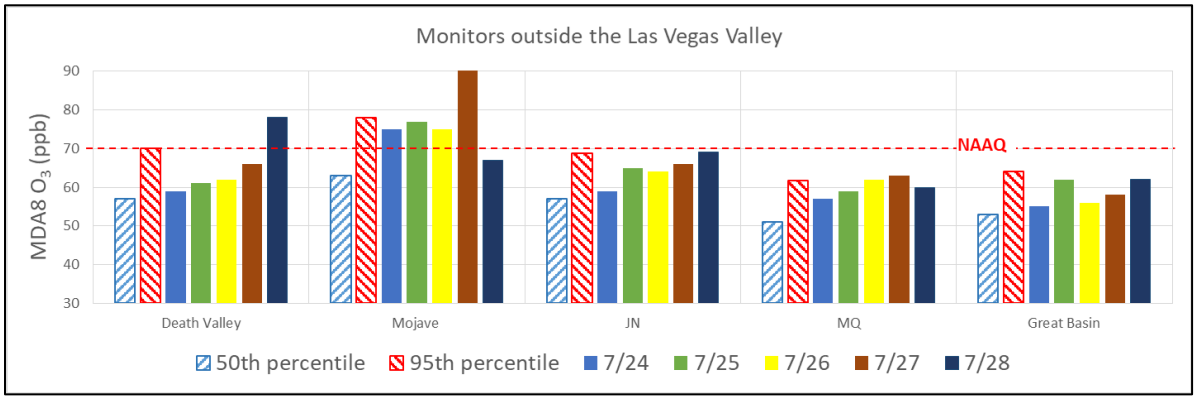

Figure 4-22. MDA8 O_3 at Monitors Outside the LVV, July 24–28, 2018.

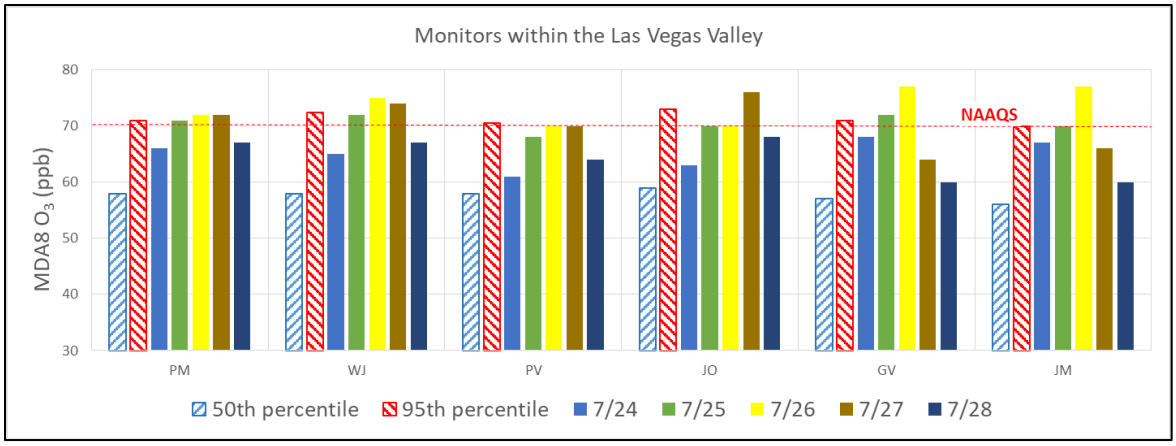

Figure 4-23. MDA8 O_3 at Monitors Inside the LVV, July 24–28, 2018.

Analysis of $PM_{2.5}$ Speciation Data

Section 4.2 describes how the ratio of $PM_{2.5}$ OC and EC can be used to differentiate combustion sources of biomass burning and mobile sources. Figure 4-23 shows actual and mean OC/EC ratios at Jerome Mack and Rubidoux, CA, and daily 24-hour $PM_{2.5}$ at Jerome Mack.

At Rubidoux, OC/EC ratios were higher than the average summer OC/EC ratio, falling in a range between 7 and 15, as defined for biomass burning. At Jerome Mack, OC/EC ratios were higher than the average summer OC/EC ratio before and after event days. Although the OC/EC ratio on July 25 for Jerome Mack was below the average summer OC/EC ratio, it was still higher than the range for gasoline (3.0–4.0) or diesel vehicles (<1.0). Therefore, these results provide evidence that wildfire emissions affected the examined monitors in the upwind area and the LVV.

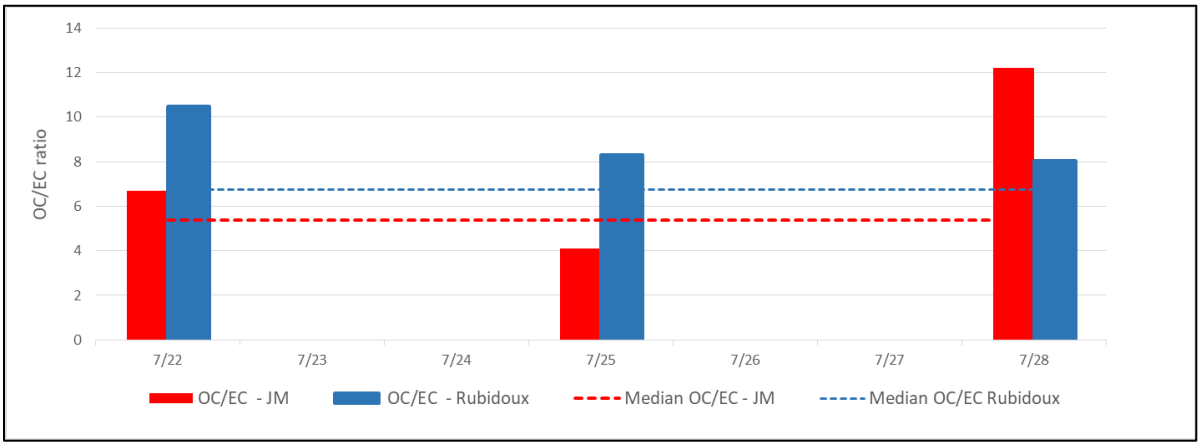

Figure 4-24. Actual and Mean OC/EC Ratio at Jerome Mack and Rubidoux, CA, and Daily 24-hour $PM_{2.5}$ at Jerome Mack, July 22–28, 2018.

Analysis of Levoglucosan

The best available $PM_{2.5}$ sample for levoglucosan analysis was collected on July 28, the day after the last event date. The analysis result was 0.004 µg/m^3 for Sunrise Acres, indicating that smoke could have been present and impacting the LVV during this event.

Supporting Ground Measurements

Ground measurements of wildfire plume components ($PM_{2.5}$, NO_2, CO) can be used to demonstrate that smoke impacted ground-level air quality if elevated concentrations or unusual diurnal patterns are observed. Jerome Mack is the only monitor that records all four pollutants, and it had the second highest exceeding ozone concentration in all of 2018 on July 26: 77 ppb.

Figures 4-24 to 4-27 present hourly levels of O_3, NO_2, $PM_{2.5}$, and CO on July 24–27; Figure 4-28 shows hourly O_3 at Mojave Desert National Park (upwind) during the same period. The intermittent smoke appears to have had a significant influence on ozone concentrations in upwind areas and the LVV. The meteorological conditions described in Section 3.3—a strong inversion and high pressure system capping the LVV—kept a large amount of ozone in the residual layer. This mixed downward after the sun rose in the morning, quickly increasing ozone concentrations.

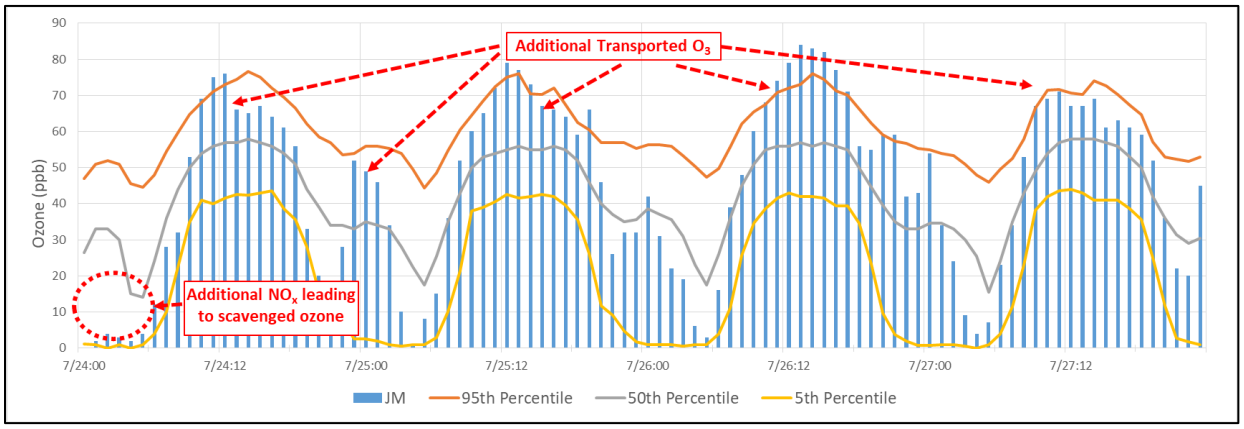

Figure 4-25. Hourly O_3 Concentrations at Jerome Mack, July 24–27.

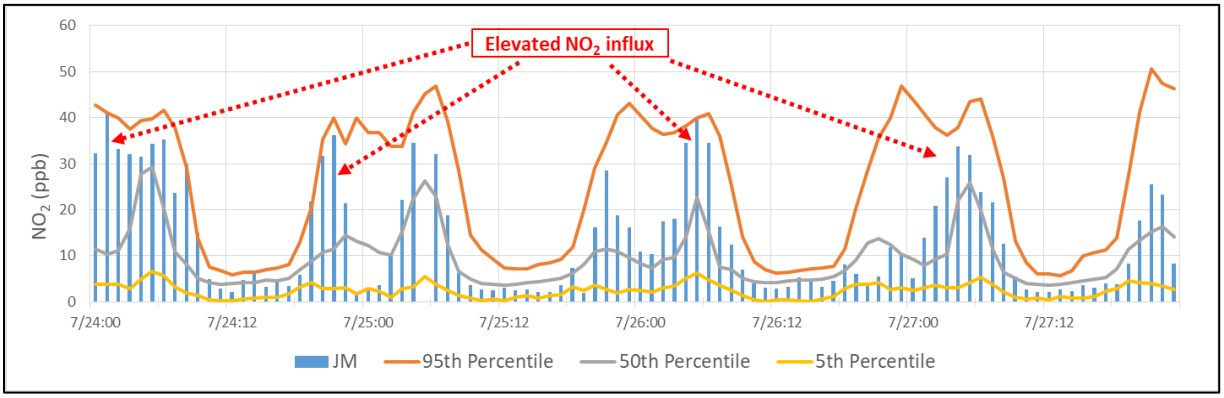

Figure 4-26. Hourly NO_2 Concentrations at Jerome Mack, July 24–27.

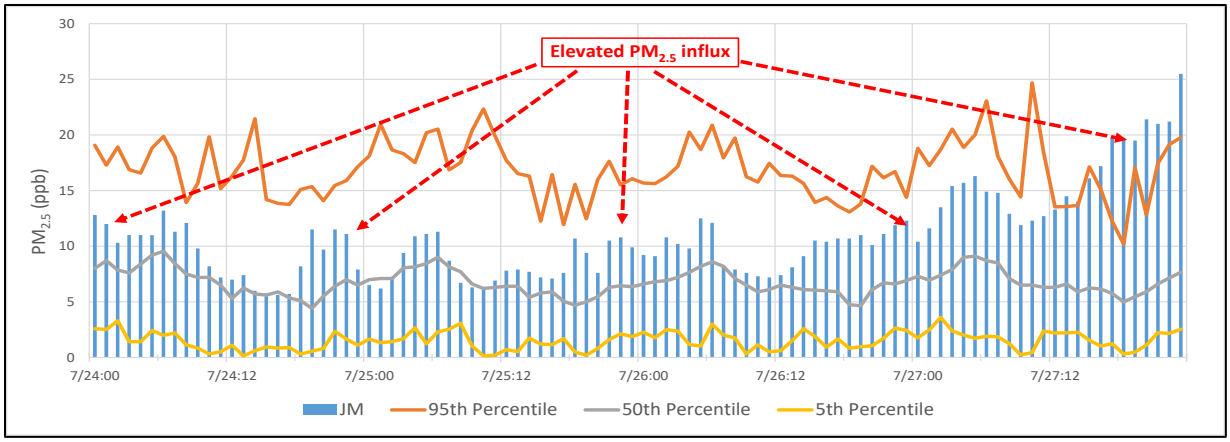

Figure 4-27. Hourly $PM_{2.5}$ Concentrations at Jerome Mack, July 24–27.

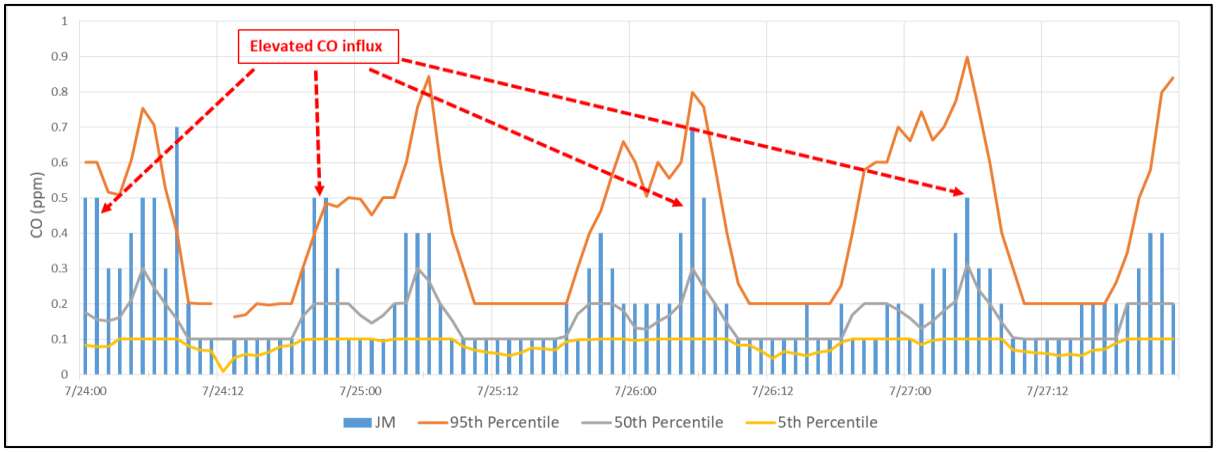

Figure 4-28. Hourly CO Concentrations at Jerome Mack, July 24–27.

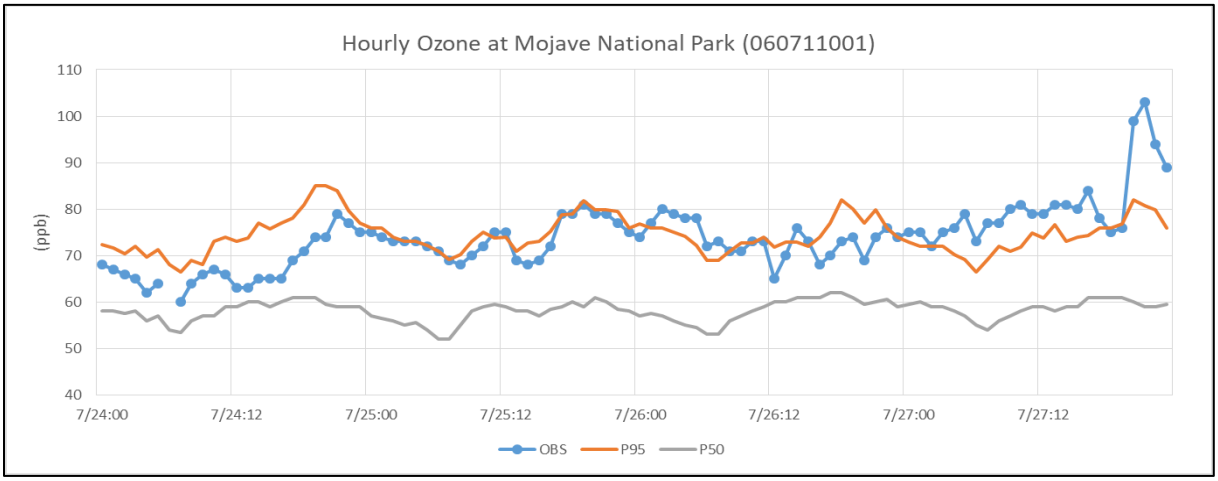

Figure 4-29. Hourly O_3 Concentrations at Mojave Desert National Park, July 24–27.

4.3.3 Tier 3 Analysis: Additional Weight of Evidence to Support Clear Causal Relationship

4.3.3.1 GAM Statistical Modeling

Figure 4-29 shows a time series of the predicted and observed MDA8 O_3 for July 24–28, 2018. The GAM prediction seems to capture the variation of observed MDA8 ozone at exceeding sites during this period relatively well. The results indicate that the monitors would normally not have exceeded the 2015 NAAQS under the meteorological conditions on July 25–27, except that the predictions for Green Valley (71 ppb) on July 26 and Joe Neal (71 ppb) on July 27 slightly exceed the 2015 NAAQS of 70 ppb due to the influence from the prior day's above-normal ozone levels (a GAM predictor). Therefore, the results suggest that a variable outside the norm (i.e., increased wildfire emissions) influenced ozone concentrations.

Table 4-1 lists GAM results for July 25–27, 2018, at exceeding monitors petitioned for data exclusion from the normal planning and regulatory requirements. GAM residuals show a modeled wildfire impact of between 1.0 and 6.0 ppb for exceeding monitors, with prediction values mostly at or below the 70 ppb standard. EPA guidance recommends using an additional step to estimate ozone contributions from wildfire: the difference between observed ozone and the sum of predicted ozone and the positive 95th percentile value. Table 4-1 shows none of the residuals exceed the 95th percentile value for July 25–27. However, two issues with this methodology must be considered.

First, a large number of wildfires affecting Clark County from 2014–2020 (especially in 2018 and 2020) included in GAM modeling cause a very conservative 95th percentile value (positive). Second, given the limitations of regression analysis for ozone production—which involves very complex physical and chemical processes regarding emissions and meteorological conditions—models are able to explain about 50% of the correlation between predicted and observed concentration (see Table 3-16 in *Exceptional Event Demonstration for Ozone Exceedances in Clark County, Nevada—June 22, 2020*), which is typical of the results seen in other regression analysis studies.

The percentile ranks of positive residuals for July 25–27 shown in Table 4-1 range from the 50th to 61st, 16th to 60th, and 28th to 65th percentiles for the exceeding monitors. The results indicate that a 39~50%, 24~84%, and 35~72% chance for the residuals at exceeding monitors would be produced under the meteorological conditions on July 25–27. The model performs more consistently on July 25, and less consistently on July 26–27, due to the influence from the prior day's above-normal ozone concentrations (a GAM predictor). This suggests other, additional emissions (e.g. wildfires) were not counted. As described in Section 3.3, the weather conditions on July 25–27 were stable and favored ozone formation. Additional wildfire emissions helped to drive already elevated ozone concentrations to exceed the 2015 ozone NAAQS.

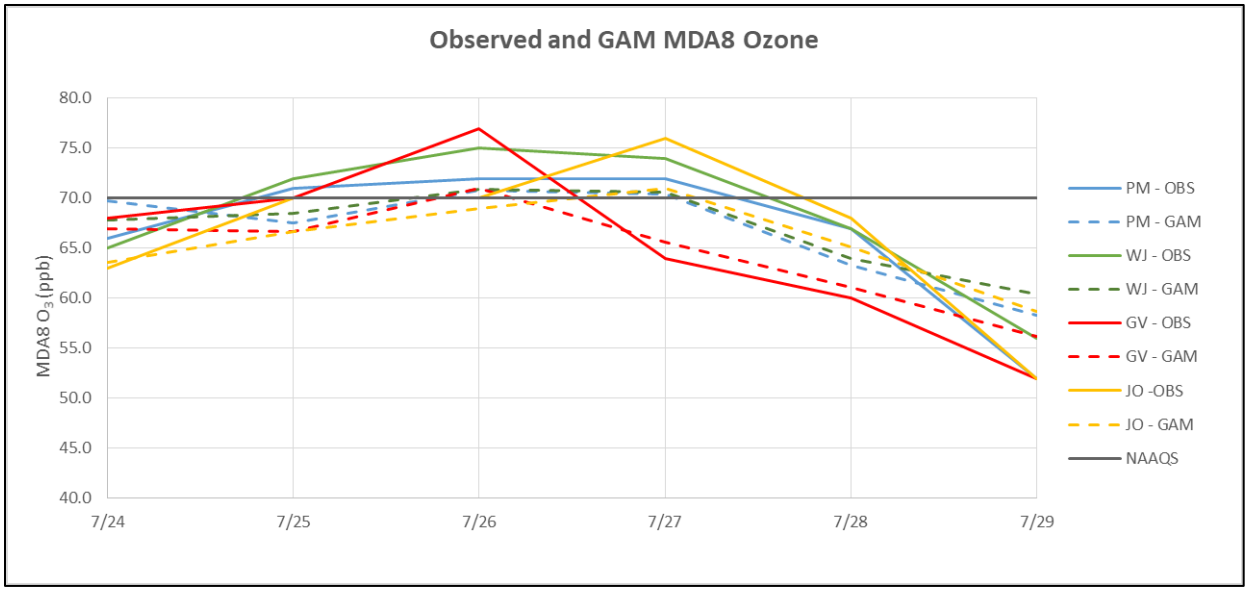

Figure 4-30. Observed and Predicted MDA8 O3 at Exceeding Monitors, July 24–29.

Table 4-1. July 25–27 GAM Results for Exceeding Sites

Date	Site	MDA8 O_3 (ppb)	MDA8 GAM Prediction (ppb)	GAM Residual (ppb)	Positive 95th Quantile (ppb)	Predicted Fire Influence	Percentile Rank of Positive Residual
7/25/2018	Paul Meyer	71	67.6	3.4	10.5	-7.1	50th
	Walter Johnson	72	68.5	3.5	10.8	-7.4	52nd
	Joe Neal	70	66.7	3.3	10.6	-7.3	51st
	Green Valley	72	67.7	4.3	10.1	-5.8	61st
7/26/2018	Paul Meyer	72	70.8	1.2	10.5	-9.4	18th
	Walter Johnson	75	70.9	4.1	10.8	-6.7	60th
	Joe Neal	70	69.0	1.0	10.6	-9.6	16th
	Green Valley	77	71.0	6.0	10.1	-4.1	76th
7/27/2018	Paul Meyer	72	70.4	1.6	10.5	-8.9	28th
	Walter Johnson	74	70.6	3.4	10.8	-7.5	51st
	Joe Neal	76	71.0	5.0	10.6	-5.6	65th

5.0 NATURAL EVENT

40 CFR 50.14(c)(3)(iv)(E) requires that agencies demonstrate an "event was a human activity that is unlikely to recur at a particular location or was a natural event." 40 CFR 50.1(k) defines a natural event as "an event and its resulting emissions, which may recur at the same location, in which human activity plays little or no direct causal role." 40 CFR 50.1(n) defines a wildfire as "any fire started by an unplanned ignition caused by lightning; volcanoes; other acts of nature; unauthorized activity; or accidental, human-caused actions, or a prescribed fire that has developed into a wildfire. A wildfire that predominantly occurs on wildland is a natural event." And lastly, 40 CFR 50.1(o) defines wildland as an "area in which human activity and development are essentially non-existent, except for roads, railroads, power lines, and similar transportation facilities. Structures, if any, are widely scattered."

Based on the documentation provided in Section 3, the events that occurred on July 25-27 fall within the definition of a natural event (40 CFR 50.1(k)). As demonstrated, these wildfires were caused by lighting or human activity and occurred predominantly on wildland, as detailed in Table 5-1, meeting the regulatory definitions outlined in 40 CFR 50.1(n) and (o). DES therefore concludes that these wildfire events can be treated as natural events under the EER.

Table 5-1. Basic Information for Wildfire Events on July 25-27, 2018

Event Date(s)	Fire	Cause	Location–County (State)
July 25-27	Ferguson	Unknown	Mariposa (CA)
	Georges	Lightning	Inyo (CA)
	Lions	Unknown	Madera (CA)
	Cranston	Unknown	Riverside (CA)
	Unnamed Mexico fires	Unknown	Mexico-CA border

6.0 NOT REASONABLY CONTROLLABLE OR PREVENTABLE

Based on the documentation provided in Section 3, lightning and human activity (as defined in 40 CFR 50.1(n)) caused the wildfires on wildland (Table 5-1) that influenced ozone concentrations in the LVV on July 25-27, 2018. DES is not aware of any evidence clearly demonstrating that prevention and control efforts beyond those actually made would have been reasonable; therefore, emissions from these wildfires were not reasonably controllable or preventable.

7.0 CONCLUSIONS

The analyses reported in this document support the conclusion that smoke from wildfires impacted ozone concentrations in Clark County, Nevada, on the event days of July 25–27, 2018. Specifically, this document has used the following evidence to demonstrate the exceptional event:

- Statistical analyses of the monitoring data compared to historical concentrations support the conclusion of unusual and above-normal historical concentrations at monitoring sites.
- Visible satellite imagery shows the spread of wildfire plumes into the LVV.
- Backward trajectories support the conclusion of transport of smoke from wildfires to LVV monitoring sites.
- Enhanced ground measurements of wildfire plume components ($PM_{2.5}$, NO_2, and CO), levoglucosan, and OC/EC ratios support the conclusion that ozone concentrations at LVV monitoring sites were impacted by smoke from wildfires.
- Aerosols in vertical profile and sounding data support the conclusion that smoke was mixed down to the surface in Clark County.
- Comparisons with non-event concentrations and GAM statistical modeling support the conclusion that ozone concentrations in Clark County were well above typical summer concentrations.

Based on the evidence presented in this package, the wildfires on July 25–27, 2018, in Clark County were natural events and unlikely to recur. The analyses described satisfy the clear causal relationship criterion for recognition as an exceptional event. Based on this evidence, DES requests that EPA exclude the data recorded at Green Valley, Joe Neal, Walter Johnson, and Paul Meyer on July 25-26, 2018, and the data recorded at the Paul Meyer, Walter Johnson, and Joe Neal monitors on July 27, 2018, from use for regulatory determinations.

8.0 REFERENCES

Bhattarai H., Saikawa E., Wan X., Zhu H., Ram K., Gao S., Kang S., Zhang Q., Zhang Y., Wu G., Wang X., Kawamura K., Fu P., and Cong Z. (2019) Levoglucosan as a tracer of biomass burning: recent progress and perspectives. *Atmospheric Research*, 220, 20-33, doi: 10.1016/j.atmosres.2019.01.004. Available at http://www.sciencedirect.com/science/article/pii/S0169809518311098.

Butler, T.J., Vermeylen F.M., Rury M., Likens G.E., Lee B., Bowker G.E., and McCluney L. 2011. "Response of ozone and nitrate to stationary source NOx emission reductions in the eastern USA." *Atmospheric Environment*, *45*(5), 1084-1094, doi:10.1016/J.Atmosenv.2010.11.040.

DES. 2008. *Southwest Desert/Las Vegas Ozone Transport Study (SLOTS).* Las Vegas, NV: Clark County Department of Environment and Sustainability.

DES. 2013. *Las Vegas Ozone Study (LVOS)*. Las Vegas, NV: Clark County Department of Environment and Sustainability.

DES. 2017. *Fires, Asia, and Stratospheric Transport Las Vegas Ozone Study (FAST-LVOS).* Las Vegas, NV: Clark County Department of Environment and Sustainability.

EPA. 2012. "Our Nation's Air: Status and Trends through 2010." U.S. Environmental Protection Agency, EPA-454/R-12-001. Research Triangle Park, NC: Office of Air Quality Planning and Standards.

EPA. 2016. "Guidance on the Preparation of Exceptional Events Demonstrations for Wildfire Events that May Influence Ozone Concentrations." U.S. Environmental Protection Agency memo. Research Triangle Park, North Carolina.

He, H. et al. 2013. "Trends in emissions and concentrations of air pollutants in the lower troposphere in the Baltimore/Washington airshed from 1997 to 2011." *Atmos. Chem. Phys.*, *13*(15), 7859-7874, doi:10.5194/acp-13-7859-2013.

Hennigan C.J., Sullivan A.P., Collett J.L., Jr., and Robinson A.L. (2010) Levoglucosan stability in biomass burning particles exposed to hydroxyl radicals. *Geophysical Research Letters*, 37(L09806), doi: 10.1029/2010GL043088. Available at https://www.firescience.gov/projects/09-1-03-1/project/09-1-03-1_hennigan_etal_grl_2010.pdf.

Hoffmann D., Tilgner A., Iinuma Y., and Herrmann H. (2009) Atmospheric stability of levoglucosan: a detailed laboratory and modeling study. *Environ. Sci. Technol.*, 44, 694–699.

Jaffe, D.A., Bertschi I., Jaegle L., Novelli P., Reid J.S., Tanimoto H., Vingarzan R., and Westphal D.L. 2004. "Long-range transport of Siberian biomass burning emissions and impact on surface ozone in western North America." *Geophys. Res. Let.*, 31(L16106).

Lai C., Liu Y., Ma J., Ma Q., and He H. (2014) Degradation kinetics of levoglucosan initiated by hydroxyl radical under different environmental conditions. *Atmos. Environ.*, 91, 32-39, doi: 10.1016/j.atmosenv.2014.03.054, 2014/07/01/. Available at http://www.sciencedirect.com/science/article/pii/S1352231014002398.

Lee, S., Baumann, K., Schauer, J.J., Sheesley, R.J., Naeher, L.P., Meinardi, S., Blake, D.R., Edgerton, E.S., Russell, A.G., Clements, M., 2005. "Gaseous and particulate emissions from prescribed burning in Georgia." *Environmental Science and Technology* 39, 9049-9056.

Lee., S., Russell, A.G., 2007. "Estimating uncertainties and uncertainty contributors of CMB PM2.5 source apportionment results." *Atmospheric Environment* 41, 9616-9624.

Lefohn, A., Shadwick D., and Oltmans S. 2010. "Characterizing changes in surface ozone levels in metropolitan and rural areas in the United States for 1980-2008 and 1994-2008." *Atmos. Environ.*, 44, 5199-5210

Nikolov, N. 2008. "Impact of Wildland Fires and Prescribed Burns on Ground Level Ozone Concentration." Paper presented at the Western Regional Air Partnership Workshop on Regional Emissions & Air Quality Modeling Studies, July 30, 2008, Denver, CO.

Pace, T.G., and Pouliot, G. 2007. "EPA's Perspective on Fire Emission Inventories—Past, Present, and Future." Paper presented at the 16th Annual International Emission Inventory Conference (*Emission Inventories: Integration, Analysis, and Communications),* May 14-17, 2007, Raleigh, NC.

Pfister, G.G., Wiedinmyer C., and Emmons L.K. 2008. "Impact of the 2007 California wildfires on surface ozone: integrating local observations with global model simulations." *Geophysical Research Letters*, 35, L19814. doi:10.1029/2008GL034747.

Pio, C.A., Legrand, M., Alves, C.A., Oliveira, T., Afonso, J., Caseiro, A., Puxbaum, H., Sanchez-Ochoa, A., Gelensser, A., 2008. "Chemical composition of atmospheric aerosols during the 2003 summer intense forest fire period." *Atmospheric Environment* 42, 7530-7543.

Rowson, D. and Colucci S. 1992. "Synoptic Climatology of Thermal Low-Pressure Systems over South-Western North America." *International Journal of Climatology*, vol. 12: 529-545.

Sonoma Technology. 2020. "Exceptional Event Demonstration for Ozone Exceedances in Clark County, Nevada—August 18-21, 2020." Section 3.3.2. Petaluma, CA: Sonoma Technology.

Stewart, J., Whiteman C., Steenburgh W., and Bian X. 2002. "A climatological study of thermally driven wind systems of the U.S. intermountain west." *Bulletin of the American Meteorological Society* 83, 699-708

Wood, S.N. 2017. *Generalized Additive Models: An Introduction with R*. 2nd edition. Boca Raton, FL: CRC Press.

Zheng, M., Cass, G.R., Ke, L., Wang, F., Schauer, J.J., Edgerton, E.S., Russell, A.G., 2007. "Source apportionment of daily fine particulate matter at Jefferson street, Atlanta, GA, during summer and winter." *Journal of the Air and Waste Management Association* 57, 228-242.